NTNU

Norwegian University of
Science and Technology

Application of Backpressure Analysis to Gas Condensate Systems

Tore Nymoen

Petroleum Geoscience and Engineering
Submission date: June 2017
Supervisor: Curtis Hays Whitson, IGP

Norwegian University of Science and Technology
Department of Geoscience and Petroleum

Preface

This thesis concludes the five year Master of Science degree in Petroleum Engineering at the Norwegian University of Science and Technology (NTNU). The fourth year of my studies was spent at the University of Oklahoma as an exchange student. The work for this thesis has been conducted during the spring semester of 2017.

I want to thank my supervisor Professor Curtis H. Whitson for providing me with the resources needed to finalize this project. This includes technical explanations, guidance, and support. His experience and feedback has been essential. I want to thank all the friends I made here in Norway and in my studies abroad. My gratitude goes out to my closest family for supporting me in all the important ways in my pursuit of higher education.

Trondheim, June 2017

Tore Nymoen

Summary

The deliverability of a natural gas well refers to its production capabilities under specific conditions and bottomhole flowing pressures. The deliverability is determined through a multipoint test, where the well is produced under a series of combinations of pressure, rates, and other data as a function of time. Results from these tests are used to generate an Inflow Performance Relationship, which determines the reservoir pressure-rate behavior for a given well. The deliverability equation for a well can be modified to include friction flow effects in tubing and pipeline, such that a single equation determines the entire pressure drop from the reservoir through the pipeline. A plot of pressure drop versus rate is often referred to as a backpressure curve.

As natural gas is produced, the pressure in the near-well region will often drop below the dewpoint pressure. This will result in an accumulation of condensate around the wellbore, and leads to decreased well deliverability. The commingled flow of both gas and liquid phases through the production tubing also increases the pressure drop encountered while lifting the fluids to surface. These effects require changes in the specific modeling of the system compared to flow of dry gas.

Backpressure curves for dry gas and gas condensate fluids have been generated using Excel VBA. By implementing a steady-state reservoir model and a tubing flow model, the pressure-rate behavior of the entire system can be investigated. The tubing flow model is based on the Gray Correlation. In order to acquire physically sound results from the tubing model for a range of production rates, the Gray Correlation is modified. Using the coupled Excel VBA model, three sets of backpressure curves have been generated, allowing for comparison of dry gas curves and gas condensate curves. The sets of curves show differences between backpressure curves for dry gas and for gas condensate. Low pressure gas condensate systems behave fairly equal to dry gas, high pressure gas condensate does not. Traditional backpressure curves can sufficiently describe pressure-rate behavior for low pressure dry gas, but not for high pressure dry gas or gas condensate. Lean and rich gas condensates behave similarly with regards to backpressure curves.

Sammendrag

Leveringsevnen til en gassbrønn referer til produksjonskapabilitetene under gitte betingelser og bunnhullstrykk. Leveringsevnen bestemmes av en flerpunktstest, hvor brønnen blir produsert under en rekke kombinasjoner av trykk, strømningsrater, og andre data som en funksjon av tid. Resultatene fra disse testene brukes til å lage Innstrømningskarakteristikk, som beskriver trykk-rate forholdet for en gitt brønn. Ligningen for leveringsevnen til en gassbrønn kan utvides til å inkludere trykkfallseffekter i produksjonsrør og transportrør, slik at én enkelt ligning beskriver trykkfallet fra reservoaret til enden av transportrøret. Et plott av trykkfall mot produksjonsrate kalles ofte for en trykkfallskurve.

Når naturgass produseres, vil trykket i nærbrønnregionen ofte bli lavere enn duggpunktstrykket til gassen. Dette fører til at væske kondenseres og akkumuleres rundt brønnen, noe som svekker leveringsevnen. I tillegg til dette øker trykkfallet i produksjonsrøret når brønnstrømmen er en blanding av både gass og væske. Disse effektene krever endring i modelleringen av produksjonssystemet sammenlignet med strømning av tørr gass.

Trykkfallskurver for tørr gass og gass-kondensat har blitt laget ved hjelp av Excel VBA. Ved å implementere en tidsuavhengig reservarmodell og en produksjonsrørmodell kan trykk-rate forholdet til hele systemet undersøkes. Produksjonsrørmodellen er basert på Gray korrelasjonen. For å få fysisk realistiske resultater fra produksjonsrørmodellen over et spektrum av produksjonsrater må Gray korrelasjonen modifiseres. Ved å bruke den koblede Excel VBA modellen har tre sett med trykkfallskurver blitt generert, slik at man kan sammenligne kurver for tørr gass og gass-kondensat. Kurvene viser forskjeller mellom oppførsel for tørr gass og gass-kondensat. Gass-kondensat ved lavt trykk oppfører seg forholdsvis likt tørr gass, i motsetning til gass-kondensat ved høyt trykk. Tradisjonelle trykkfallskurver kan beskrive trykk-rate oppførsel for tørr gass ved lave trykk, men ikke for tørr gass eller gass-kondensat ved høyt trykk. Magre og rike gass-kondensatfluider oppfører seg forholdsvis likedan med tanke på trykkfallskurver.

Contents

List of Figures

List of Tables

Chapter 1

Introduction

Norway's revenue from natural gas exports are, for the first time in history, close to exceeding the revenue from exports of oil. As a matter of fact, due to the low oil price of 2015, gas export revenue was 10% higher than oil export revenue. This is shown in **Fig. 1.1**. On a global scale, natural gas demand is expected to increase with 1.6% per annum. Environmental requirements are putting pressure on coal consumption, allowing for natural gas to fill the void left behind from less use of coal. Natural gas is set to overtake coal as the second largest fuel source by 2035, and gas from shale production is expected to account for around 60% of the increase in natural gas supply. In addition to this, the world economy is expected to double over the next 20 years, as more than 2 billion people are lifted out over poverty. (BP, 2017). These reasons show how natural gas production is important today, and will be even more important in the future.

1.1 Background

Estimating the value and the potential of a production well is crucial. Determining the production potential, or deliverability, of a natural gas well is usually done through a backpressure test. The result of a backpressure test is a relationship between pressure and production rate. This relationship is one of the factors that are used to determine the value of a well. The relationship between pressure and production rate is well known for wells producing minimal amount of liquids, usually referred to as "dry gas".

For natural gas wells producing significant amounts of liquids (further referred to as "gas con-

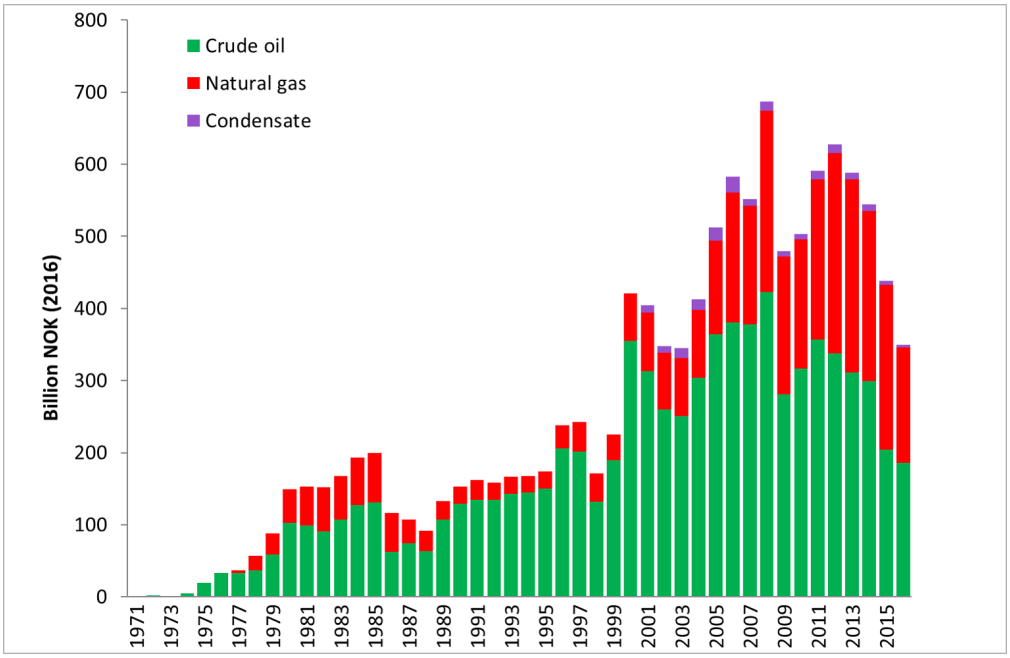

Figure 1.1: Norway's export revenue from sales of petroleum products. Data retrieved from Norsk Petroleum (2017).

densate wells"), the relationship between pressure and production rate is more complex. The reasons for this are mainly condensation of liquid in the reservoir, and higher pressure drop while lifting the fluids to surface. Both these effects are negative. The magnitude of these negative effects are important to understand in order to accurately predict the performance of a gas condensate well. A positive effect from producing condensate from a natural gas well is that the sellable liquids at the surface add value to the well. The sales price of liquid is much higher than the sales price of gas.

In order to estimate the negative effects of producing gas condensate, this thesis is highly influenced by Mike Fetkovich's work on dry gas well deliverability. Dry gas well deliverability is essential to understand before analyzing gas condensate well deliverability. To determine the performance of gas condensate reservoirs the calculation method developed by Øyvind Fevang and Curtis H. Whitson is incorporated. Vertical lifting performance is determined using the Gray Correlation, developed by H.E. Gray of Shell Oil Company in the 1950's.

This thesis provides an indication, through the use of backpressure curves, of the magnitude of the negative effects attributed to gas condensate production. The negative effects are shown qualitatively, but quantification of these effects are not the scope of this thesis.

1.2 Objectives

The main objectives of this Master's project are

1. To build a steady-state reservoir model for dry gas, for a lean gas condensate fluid, and for a rich gas condensate fluid.
2. To build the Gray Correlation as a tubing model applicable for dry gas and gas condensate wells.
3. To incorporate the reservoir and the tubing model into a coupled steady-state well model, that is able to describe the behavior of the entire system.
4. To present deliverability curves for low and high pressure gas reservoirs according to the theory presented by Mike Fetkovich.
5. To present deliverability curves for the two gas condensate fluids.
6. To compare deliverability curves for dry gas systems and gas condensate systems.

1.3 Structure of the Report

The rest of the report is organized as follows. Chapter 2 gives an introduction to the governing theory concerning dry gas well deliverability. Chapter 3 describes the special considerations required in modelling gas condensate wells. Chapter 4 is a description of how the reservoir and the tubing model was made using Excel VBA. Chapter 5 presents backpressure curves that were created using the coupled model. Chapter 6 presents conclusions. Limitations and recommendations for future work is presented in Chapter 7.
Chapter 2 and 3 are based on work done during the fall of 2016. Most of these two chapters were part of my project work in *TPG4560 - Petroleum Engineering, Specialization Project.*

Chapter 2

Dry Gas Well Deliverability

Deliverability testing refers to the testing of a gas well to measure its production capabilities under specific conditions and bottomhole flowing pressures. A common objective of a deliverability test is the absolute open-flow (AOF) of a well. The AOF is the maximum rate at which a well could flow against a theoretical atmospheric backpressure at the sandface (Lee and Wattenbarger, 1996). Another application of the deliverability test is to help generating an Inflow Performance Relationship (IPR) for the well. The IPR describes the relationship between the production rate and the bottomhole flowing pressure at a given reservoir pressure.
This chapter gives an introduction to the different types of deliverability tests, specific applications, and a brief overview of the theory behind the governing equations used in deliverability calculations.

2.1 Introduction to Gas Flow

The generalized diffusivity equation for radial flow of real gas through a homogenous, isotropic porous medium is given as (Lee and Wattenbarger, 1996)

$$\frac{1}{r}\frac{\partial}{\partial r}\left(r\frac{p}{\mu_g z}\frac{\partial p}{\partial r}\right)\frac{1}{0.0002637} = \frac{\phi c_t p}{k_g z}\frac{\partial p}{\partial t}. \tag{2.1}$$

Equation (2.1) is non-linear, but is linearized with the real gas pseudopressure transformation

$$p_p(p) = 2\int_{p_0}^{p} \frac{p}{\mu_g z} dp. \tag{2.2}$$

Using the pseudopressure transformation, Eq. (2.1) can be solved without assuming that certain gas properties are constant with pressure. The pseudopressure function is shown in **Fig. 2.1**. Note that as pressure is lower than 2000 psia, the pseudopressure function is approximately linear with pressure. The integral can therefore be simplified to

$$p_p(p) = 2\int_{p_0}^{p} \frac{p}{\mu_g z} dp \approx \frac{p^2 - p_0^2}{(\overline{\mu_g z})}. \tag{2.3}$$

Further on, this is referred to as the "pressure squared" solution. This result is convenient for low pressure reservoirs. We also observe that as pressure is "high" (>2000psia), $(p/\mu_g z)$ is approximately constant. A common simplification of the pseudopressure function is then

$$p_p(p) = 2\int_{p_0}^{p} \frac{p}{\mu_g z} dp \approx \frac{p}{\mu_g z}(p - p_0). \tag{2.4}$$

2.2 Well Deliverability Testing

In order to determine the deliverability of a well, it has to be tested with a multipoint test. A multipoint test consists of measuring a series of pressures, rates, and other data as a function of time (Fetkovich, 1975). These tests are often required for other purposes as well, such as by state regulatory bodies or simply information gathering for reservoir and production engineering studies. There are two basic types of multipoint tests:

1. Flow After Flow Test (No shut-in between flows)
   (a) Normal sequence
   (b) Reverse sequence

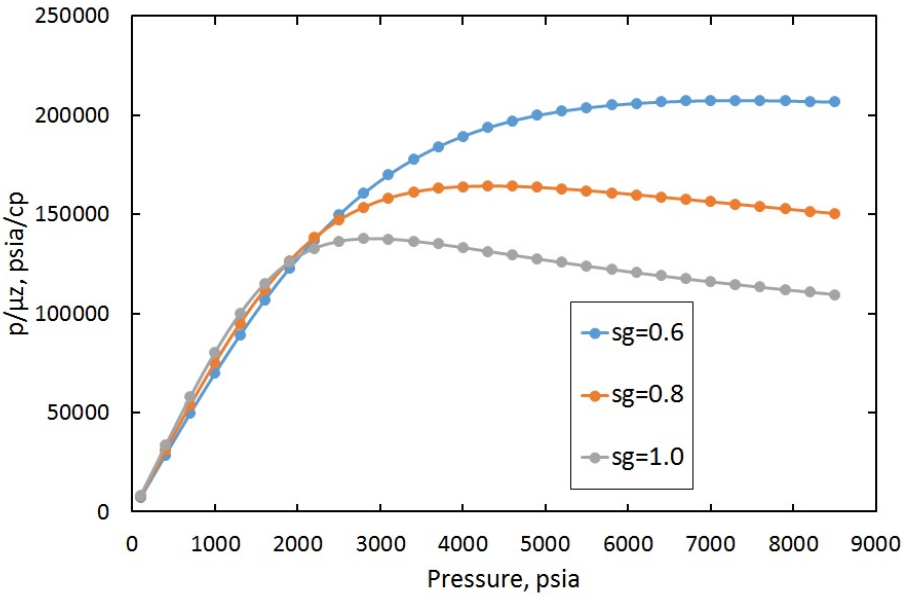

Figure 2.1: Pseudopressure function

2. Isochronal Test (Well is shut-in between flows)

   (a) Standard Isochronal

   (b) Modified Isochronal

2.2.1 Flow After Flow Tests

The flow after flow test is often referred to as the "four-point test", since it is common for regulatory bodies to require testing at four different rates. The test is performed by producing the well at a series of *stabilized* rates and obtaining the corresponding stabilized flowing bottomhole pressure (Petrowiki, 2015a). The test is started from a shut-in condition, and flow rates may be increasing (normal sequence) or decreasing (reverse sequence). There is no shut-in between flow periods.

2.2.2 Isochronal Tests

Standard isochronal tests are done by having a number of equally timed flow periods starting at comparable shut-in conditions. This usually refers to having a shut-in bottomhole pressure

equal to the average reservoir pressure. This method of testing takes advantage of the principle that radius of investigation is a function of the flow period and not the flow rate (Lee and Wattenbarger, 1996). It follows that a stabilized rate during the flow period is not necessary to have a valid isochronal test. A disadvantage of the (standard) isochronal test is the time required for the bottomhole pressure to build up to the average reservoir pressure. The Modified isochronal test tries to mitigate this problem by having shut-in periods of similar duration as the flowing periods.

2.3 Reservoir Deliverability Curve

The late time or pseudosteady-state soluton to Eq. (2.1) for constant rate production, assuming closed outer boundaries, is given as

$$p_p(p_R) - p_p(p_{wf}) = \frac{1.422 \times 10^6 qT}{k_g h} \times \left[1.151 log\left(\frac{10.06A}{C_A r_w^2} \right) - 3/4 + s + Dq \right]. \tag{2.5}$$

We define the parameters A_{bh} and B_{bh}

$$A_{bh} = \frac{1.422 \times 10^6 T}{k_g h} \times \left[1.151 log\left(\frac{10.06A}{C_A r_w^2} \right) - 3/4 + s \right], \tag{2.6}$$

$$B_{bh} = \frac{1.422 \times 10^6 TD}{k_g h}, \tag{2.7}$$

such that Eq. (2.5) simplifies to

$$p_p(p_R) - p_p(p_{wf}) = A_{bh} q + B_{bh} q^2 \tag{2.8}$$

which is the theoretical bottomhole deliverability equation, and q is the well surface gas rate. Equivalent solutions can be derived for both the transient solution and the pressure squared formulation.

By dividing both sides of the equation with q, we obtain

$$\frac{p_p(p_R) - p_p(p_{wf})}{q} = A_{bh} + B_{bh} q \tag{2.9}$$

A cartesian plot of $(p_p(p_R) - p_p(p_{wf}))/q$ vs. q from a back-pressure test will then yield A_{bh} from the intersection and B_{bh} from the slope. This is often referred to as the *Houpert Analysis Technique*. When these coefficients are determined, the AOF can be calculated by means of Eq. (2.8) with p_{wf} equal to atmospheric pressure.

2.4 Empirical Deliverability Equations

The empirical deliverability relationship for low pressure reservoirs (< 2000 psia) is given as

$$q = C\left(p_R^2 - p_{wf}^2\right)^n = C\left(\Delta p^2\right)^n. \tag{2.10}$$

In terms of pseudopressure, (2.10) becomes

$$q = C\left(p_p(p_R) - p_p(p_{wf})\right)^n = C\left(\Delta p_p\right)^n, \tag{2.11}$$

which is valid for all pressure ranges. C is the stabilized flow coefficient, and n is the inverse slope of the line on a log-log plot of either Δp^2 or Δp_p vs. gas flow rate. Taking the logarithm of both sides of Eq. (2.11) we obtain the equation that forms the basis for *Rawlins-Schellhardt Analysis*

$$log(q) = log(C) + n \times log(\Delta p_p). \tag{2.12}$$

Since we usually plot Δp_p vs. q rather than the opposite, we rearrange the equation such that

$$log(\Delta p_p) = \frac{log(q)}{n} - \frac{loq(C)}{n}. \tag{2.13}$$

If we then plot Δp_p vs. q on log-log scales we will get a straight-line with a slope of $1/n$ and an intercept of $-log(C)/n$. The value of n depends on the flowing conditions. For turbulent non-Darcy flow, n is close to 0.5. If flow behavior is laminar, that is to say described by Darcy's equation, n is close to 1.0. (Lee and Wattenbarger, 1996).

2.5 Deliverability curves at surface datum

The deliverability relation in Eq. (2.8) gives us a relationship between bottomhole pressures and rate for a given well. It is convenient to modify this relation to acquire a relationship between wellhead pressures and rate. Let p_c be the wellhead shutin pressure, and p_w the wellhead static column flowing pressure. p_w is the pressure that would be recorded on the annulus while flowing if there was no packer in the well (Fetkovich, 1975). Define the wellhead deliverability equation

$$p_p(p_c) - p_p(p_w) = A_{wh}q + B_{wh}q^2. \tag{2.14}$$

This equation is valid for both high and low pressure reservoirs. As an approximation for low pressure systems, the hydrostatic head term e^S is used to relate bottomhole and wellhead pressures. S is defined as

$$S = \frac{0.0375\gamma_g h}{\bar{z}\bar{T}}. \tag{2.15}$$

The hydrostatic head term is based upon the *Average Temperature and z-Factor method* (described more in Section 2.6), and is usually solved as an iterative process (Lee and Wattenbarger, 1996). If we define $p_c^2 = p_R^2/e^S$ and $p_w^2 = p_{wf}^2/e^S$, Eq. (2.8) is simplified to the common wellhead pressure-squared deliverability equation for low pressures

$$p_c^2 - p_w^2 = \frac{A_{bh}}{e^S}q + \frac{B_{bh}}{e^S}q^2 = A'_{wh}q + B'_{wh}q^2. \tag{2.16}$$

The empirical deliverability relationship in Eq. (2.11) can also be utilized, such that

$$q = C_{wh}(p_p(p_c) - p_p(p_w))^n. \tag{2.17}$$

Note that the value of C and n will differ from the values found using bottomhole pressures. It is also perfectly valid to use pressure-squared rather than pseudopressure in Eq. (2.17).

2.6 Tubing Friction Effects

The pressure drop experienced in lifting reservoir fluids to surface is one of the main factors affecting well deliverability. As much as 80% of the total pressure loss in a flowing well may occur

during flow through tubing to the surface (Petrowiki, 2015c). There are several different methods used to calculate the frictional pressure drop in a gas well. A common method is the *Average Temperature and z-Factor method*. A variant of this method is presented by Mike Fetkovich Fetkovich (1975). The Fetkovich equation is given in Appendix A. The Average Temperature and z-Factor method give the following relationship between bottomhole flowing pressure p_{wf} and wellhead flowing tubing pressure p_t.

$$p_{wf}^2 = p_t^2 e^S + \frac{6.67 \times 10^{-4} q^2 f \bar{T}^2 \bar{z}^2}{d^5 \cos\theta}(e^S - 1). \tag{2.18}$$

Rewrite the equation to get all pressure terms on the left side and divide by e^S

$$\frac{p_{wf}^2}{e^S} - p_t^2 = \frac{6.67 \times 10^{-4} q^2 f \bar{T}^2 \bar{z}^2}{d^5 \cos\theta} \frac{(e^S - 1)}{e^S}. \tag{2.19}$$

Know that $p_{wf}^2 / e^S = p_w^2$. Simplify the equation further, such that

$$p_w^2 - p_t^2 = T_{wh} q^2, \tag{2.20}$$

where

$$T_{wh} = \frac{6.67 \times 10^{-4} \bar{T}^2 \bar{z}^2}{d^5 \cos\theta} \frac{(e^S - 1)}{e^S}. \tag{2.21}$$

Eq. (2.20) will plot as a straight line in a log-log plot with a slope of 0.5 (Fetkovich, 1975).
It is important to note that it will not easily transform to a useful pseudopressure relation. However, if we assume that the pressure-squared solution is valid, we come up with some interesting relations.

2.6.1 Pressure-Squared Relations

We continue with Eq. (2.14) assuming that pressure is "low", which means that the pseudopressure function may be approximated by the pressure-square solution as shown in Eq. (2.16). The wellhead backpressure equation is then

$$p_c^2 - p_w^2 = A'_{wh} q + B'_{wh} q^2 \tag{2.22}$$

The coefficients are denoted A'_{wh} and B'_{wh} to clarify that they differ from the coefficients found when having the wellhead backpressure equation on pseudopressure form.
We then add Eq. (2.20) and Eq. (2.22), and obtain the wellhead backpressure equation that accounts for the total pressure drop through the reservoir and the tubing

$$(p_c^2 - p_w^2) + (p_w^2 - p_t^2) = A'_{wh}q + B'_{wh}q^2 + T_{wh}q^2 \tag{2.23}$$

or

$$(p_c^2 - p_t^2) = A'_{wh}q + (B'_{wh} + T_{wh})q^2, \tag{2.24}$$

which can also be represented with the empirical deliverability equation as

$$q = C_{wht}(p_c^2 - p_t^2)^n. \tag{2.25}$$

Note that when the tubing friction loss given by T_{wh} is very large compared to A'_{wh} and B'_{wh}, n approaches 0.5 (Fetkovich, 1975). The system is then said to be *tubing limited*. If the pressure drop in the tubing is insignificant n will be approximately equal to 1.0.

2.7 Pipeline pressure drop effects

The total system pressure drop can be elaborated further if we continue with the pressure-squared solution. There are several different equations relating flowrate and pressure drop in a pipeline, including the *Weymouth, Panhandle, Spitzglass*, and others (Petrowiki, 2015b). For simplicity, the concept will be shown using the Weymouth equation. This equation is used for flows with high Reynolds number where the Moody friction factor is merely a function of the relative roughness of the pipe. Weymouth's equation is given as

$$q = 1.1d^{2.67}\left(\frac{p_{up}^2 - p_{dwn}^2}{L\gamma_g z T_{in}}\right)^{0.5}. \tag{2.26}$$

We assume that the gathering line is connected to the tubing, such that $p_{up} = p_t$. Square both sides of the equation and rearrange, and get

$$p_t^2 - p_{dwn}^2 = \frac{L\gamma_g z T_{in}}{1.21 d^{5.34}} q^2. \tag{2.27}$$

We then define

$$L_{wh} = \frac{L\gamma_g z T_{in}}{1.21 d^{5.34}}, \tag{2.28}$$

such that we end up with

$$p_t^2 - p_{dwn}^2 = L_{wh} q^2. \tag{2.29}$$

If we then combine this equation with Eq. (2.24), we get

$$(p_c^2 - p_t^2) + (p_t^2 - p_{dwn}^2) = A'_{wh} q + (B'_{wh} + T_{wh} + L_{wh}) q^2, \tag{2.30}$$

or simply

$$(p_c^2 - p_{dwn}^2) = A'_{wh} q + (B'_{wh} + T_{wh} + L_{wh}) q^2 \tag{2.31}$$

which now is a single equation describing the entire pressure drop from the reservoir through the pipeline.

This can of course also be represented using the empirical deliverability equation

$$q = C_{tot} (p_c^2 - p_{dwn}^2)^n. \tag{2.32}$$

By examining the individual pressure drop components, we see that for wells with large bottomhole potentials, n will approach 0.5. For small potential wells the slope would approach the slope of the bottomhole or Darcy flow curve is equal to 1.0 (Fetkovich, 1975). A slope near 1.0 means that the pressure drop in the reservoir is the dominant pressure drop.

2.8 A Note on the Different Backpressure Curves

Backpressure analysis have been utilized by the petroleum industry since the early 1900's. Initial natural gas developments were lower pressure reservoirs than those that are being produced

today, which meant that the pressure squared formulation was sufficient. The pressure squared formulation is also significantly easier to use than calculating the gas pseudopressure integral. It is no wonder that plotting Δp^2 vs. q became the industry standard rather than Δp_p vs. q. As mentioned in section 2.6 there is also no pseudopressure formulation of the relationship between tubing pressure and flowing bottomhole pressure, meaning that the wellhead static column curve cannot be easily combined with the tubing friction curve. All these factors mean that throughout this thesis backpressure curves will be presented on the pressure squared form. The following table provides a reference of the naming used for the different deliverability curves.

Table 2.1: Naming convention for backpressure/deliverability curves

Pressure relation	Curve name
$p_R^2 - p_{wf}^2$	Bottom hole
$p_c^2 - p_w^2$	Static column
$p_w^2 - p_t^2$	Tubing friction
$p_c^2 - p_t^2$	Wellhead flowing
$p_c^2 - p_{dwn}^2$	Total curve

Chapter 3

Gas Condensate Well Modelling

3.1 Introduction to Gas Condensate

A reservoir fluid is formally classified as gas condensate when the reservoir temperature is greater than the critical temperature but less than the cricondentherm. Retrograde gas-condensate reservoirs typically exhibit OGR's from about 5 - 350 STB/MMscf (GOR's between 3,000 and 150,000 scf/STB). Liquid gravities are usually between 40 and 60 °API. (Whitson and Brulé, 2000). The surface condensate adds substantial value compared to dry gas, but can potentially cause a decline in well productivity.

3.2 Three-region Flow Model

When the bottomhole flowing pressure (BHFP) drops below the dewpoint, condensate drops out near the wellbore. This results in reduced gas permeability and lower gas deliverability (Fevang and Whitson, 1995). The way to model this problem is by separating the reservoir into three distinct flow regions. These regions are shown graphically in **Fig. 3.1**.
For a given producing condition, one, two, or all three regions may exist. Each of the three regions have distinct characteristics (Fevang and Whitson, 1995).

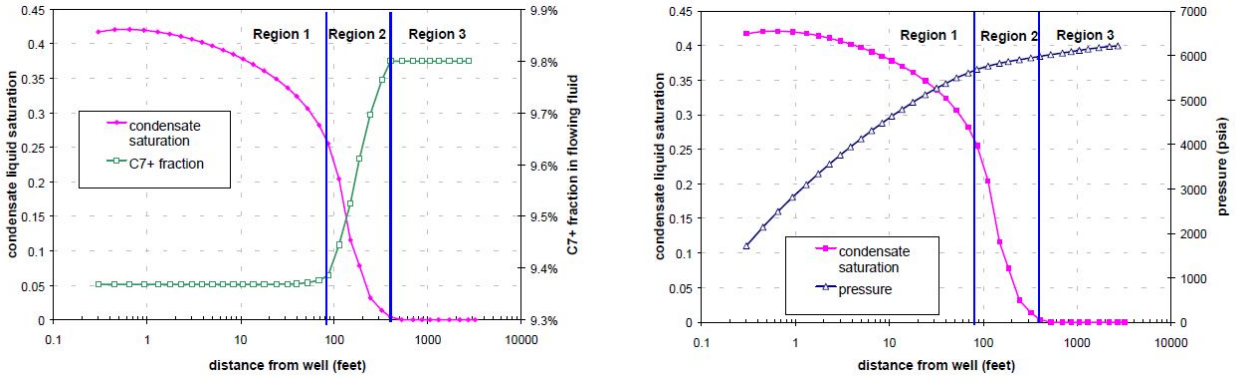

Figure 3.1: Three-region reservoir model (Mott, 1999)

Region 1 A near-wellbore region where both gas and oil flow simultaneously. Region 1 is the main source of deliverability loss in a gas condensate well. Gas relative permeability is reduced due to condensate buildup. The flowing composition is constant, such that the single-phase gas entering Region 1 has the same composition as the produced wellstream mixture. The dewpoint of the producing wellstream mixture equals the reservoir pressure at the outer edge of Region 1. The size of this region grows with time.

Region 2 A region of condensate buildup where only gas is flowing. Oil mobility is zero since the oil saturation is below the critical oil saturation needed to flow. The size of Region 2 is largest at early times just after the reservoir pressure drops below the dewpoint. It then decreases in size with time since Region 1 is expanding.

Region 3 A region containing single phase (original) reservoir gas. This region only exists in an undersaturated gas condensate reservoir. Flowing composition in this region is equal to the original reservoir gas.

3.3 Two-Phase Pseudopressure

The traditional pseudopressure function in Eq. 2.2 has to be modified to account for the three different flow regions and their different flowing phases. First we define the dry gas formation volume factor

$$B_{gd} = \frac{V_g}{V_{g,sc}} = \left(\frac{p_{sc}}{T_{sc}}\right)\left(\frac{zT}{p}\right)\left(\frac{1}{F_{\bar{g}g}}\right). \tag{3.1}$$

The total pseudopressure integral, including flow of both oil and gas in three regions is then

$$\Delta p_p(p) = \int_{p_{wf}}^{p_R} \left(\frac{k_{rg}}{B_{gd}\mu_g} + \frac{k_{ro}}{B_o\mu_o}R_s\right)dp. \tag{3.2}$$

Break this integral into three parts, such that

$$\begin{aligned}\Delta p_p(p) = \int_{p_{wf}}^{p_R} \left(\frac{k_{rg}}{B_{gd}\mu_g} + \frac{k_{ro}}{B_o\mu_o}R_s\right)dp \quad &= \\ \int_{p_{wf}}^{p^*} \left(\frac{k_{rg}}{B_{gd}\mu_g} + \frac{k_{ro}}{B_o\mu_o}R_s\right)dp \quad &+ \\ \int_{p^*}^{p_d} \frac{k_{rg}}{B_{gd}\mu_g}dp \quad &+ \\ \int_{p_d}^{p_R} \frac{k_{rg}(S_{wi})}{B_{gd}\mu_g}dp &\end{aligned} \tag{3.3}$$

where p^* is the dewpoint of the wellstream, k_{ri} is the relative permeability of the gas or the condensate phase, B_o is the oil formation volume factor, and R_s is the solution GOR. Given the producing GOR R_p, the dewpoint of the wellstream p^* is found by locating the pressure in the PVT table in which $r_s = 1/R_p$. When R_p and p^* is known one can calculate the pseudopressure integral (Fevang and Whitson, 1995).

Region 1 Calculation

At pressures lower than p^* the saturated PVT properties ($R_s, B_o, r_S, B_{gd}, \mu_o, \mu_g$) are found directly from the reservoir fluid's black oil table. This is used to calculate k_{rg}/k_{ro} as a function of pressure with the equation

$$\frac{k_{rg}}{k_{ro}} = \left(\frac{R_p - R_s}{1 - r_s R_p}\right)\frac{\mu_g B_{gd}}{\mu_o B_o}. \tag{3.4}$$

Combining this ratio with relative permeability data from specially designed experiments (Øyvind Fevang, 1995), one can calculate oil and gas relative permeability as a function of pressure. This data is then used to calculate the two-phase pseudopressure integral for Region 1.

Region 2 Calculation

In Region 2 only gas is mobile, so there is no need to acquire oil relative permeability data. There is however significant oil saturation, S_o, in this region. The Region 2 integral is evaluated by calculating $k_{rg} = f(S_o)$ by using relative oil volumes from a Constant Volume Depletion (CVD) test, or by estimating relative oil volumes with the three following equations

$$(V_{ro,CVD})_k = \frac{N_{k-1} - G_{k-1}(r_s)_k}{1-(r_s R_s)_k}(B_o)_k \tag{3.5}$$

$$N_{k-1} = \left(\frac{V_{ro,CVD}}{B_o} + \frac{1-V_{ro,CVD}}{B_{gd}} r_s\right)_{k-1} \tag{3.6}$$

$$G_{k-1} = \left(\frac{V_{ro,CVD}}{B_o} R_s + \frac{1-V_{ro,CVD}}{B_{gd}}\right)_{k-1}. \tag{3.7}$$

The oil saturation as a function of pressure is then simply $S_o = V_{ro,CVD}(1-S_w)$. The subscripts k and $(k-1)$ refer to the current and previous pressure of evaluation, respectively. $k_{rg} = f(S_o)$ is known from the relative permeability experiments mentioned in the previous subsection, thus allowing for calculating the two-phase pseudopressure integral for Region 2.

Region 3 Calculation

Throughout Region 3 the reservoir is undersaturated. This means that $k_{rg} = 1$, and the traditional single-phase gas pseudopressure formulation can be used.

3.4 Condensate Blockage

As condensate builds up in Region 1, the relative permeability of gas is reduced. This is the effect that is usally referred to as *Condensate Blockage*. As a first order approximation, one might define the condensate blockage skin as

$$s_{cb} = \left(\frac{k_{rg}}{k_{rgb}} - 1\right) ln\,(r_b/r_w)\,, \tag{3.8}$$

where k_{rgb} is the relative permeability of gas in the blockage region, r_b is the radius of the blockage region, and r_w is the wellbore radius. The magnitude of the condensate blockage skin is

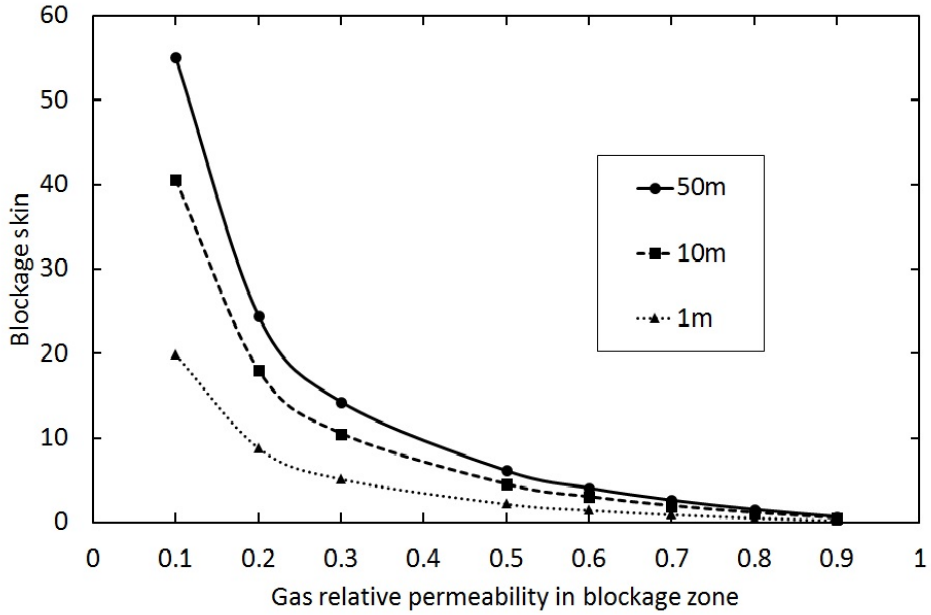

Figure 3.2: Blockage skin as a function of the radius of the blockage region

shown in **Fig. 3.2**.The loss in Productivity Index, J, is found by taking the ratio of the productivity index of a well with condensate blockage and a well without condensate blockage. The theoretical pseudosteady-state flow equation of a gas well is given in Eq. (2.5). If we assume that non-Darcy effects are negligible and that the drainage area is radial, the pseudosteady-state J simplifies to

$$J = \frac{k_g h}{1.422 \times 10^6 T \times [ln(r_e/r_w) - 3/4 + s]} = \frac{q}{p_p(p_R) - p_p(p_{wf})}. \tag{3.9}$$

The ratio of a well with blockage to a well without blockage is then

$$\frac{J_{blockage}}{J_{undamaged}} = \frac{ln(r_e/r_w) - 3/4}{(r_e/r_w) - 3/4 + s_{cb}}. \tag{3.10}$$

This condensate blockage skin then allows us to use the single phase pseudopressure relation with s_{cb} to calculate the rate of the well. Other relations exist that take into account the time dependency of the size of the blockage region (Fetkovich, 1973). As seen in Fig. 3.2, the blockage skin is higher than 10 in the majority of the cases where k_{rgb} is less than 0.3. A blockage skin of 10 accounts for more than a 50% reduction in PI according to Eq. 3.10. It is very rare to see a

reduction in PI higher than this, even though it is apparent that the blockage skin may be much higher than 10. This can be explained by the *velocity stripping effect*. In the near wellbore region where flow velocities are high, there is an improvement in k_{rg} as the liquid phase is stripped out. This effect is quantified through capillary number (the ratio of viscous to capillary forces) dependent models for relative permeability in the gas phase (Pope et al., 2000).

The complete effect of condensate blockage is found by following the calculation method described in Section 3.3. As seen in the Reservoir Rate Equation (Eq. 2.5) the gas rate is proportional to the pseudopressure integral. Using the notation in Eq. 3.2, and ignoring the effect of oil, the pseudopressure integral is essentially the area under the $(k_{rg}/B_{gd}\mu_g)$ curve. The two-phase pseudopressure calculation procedure captures the pressure dependency of k_{rg} in Region 1 and Region 2. The effect of condensate blockage on gas rates can be substantial, as shown in **Fig. 3.3**.

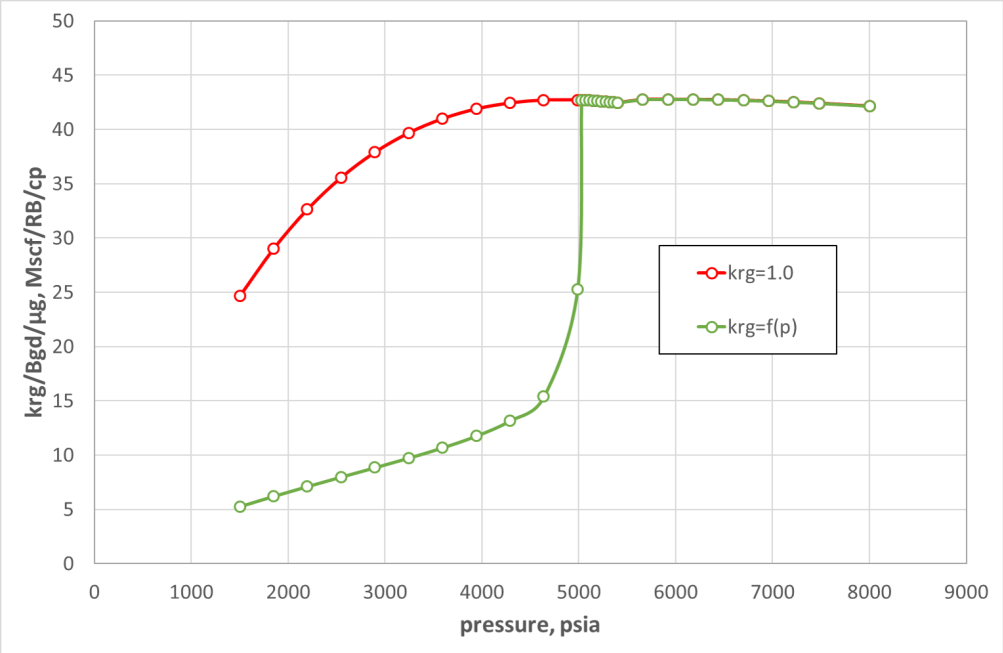

Figure 3.3: Pseudopressure function for k_{rg}=1 and for k_{rg}=f(p). The curves are generated using the same fluid properties, meaning that the difference stems from relative permeability reduction only. The fluid here is a lean gas condensate (r_{si}=45 STB/MMscf) with a dewpoint of 5400 psia. k_{rg}=1 is analogous to calculation of single phase dry gas pseudopressure.

3.5 Tubing Flow Performance

The overall flow performance through the tubing is affected by the condensate dropout. Multiphase flow behavior depends strongly on the distribution of the phases in the pipe, which in turn depends on the inclination of the well (Economides et al., 2013). This has strong implications on the pressure drop through the tubing and therefore bottomhole flowing pressure (BHFP).
A common technique for including the effects of liquid production is modification of the gas gravity term to account for the additional fluid density caused by the presence of liquids. This technique is only valid for producing gas/liquid ratios in excess of 10,000 scf/STB (Lee and Wattenbarger, 1996). Richer reservoir fluids require two-phase correlations for calculating BHFP. The most common two-phase correlations are *Hagedorn and Brown*, *Griffith*, *Beggs and Brill*, and *The Gray Correlation*. The correlations are based on mechanical energy balance. The mechanical energy balance on differential form is given as

$$\frac{\partial p}{\partial z} = \left(\frac{\partial p}{\partial z}\right)_{PE} + \left(\frac{\partial p}{\partial z}\right)_{KE} + \left(\frac{\partial p}{\partial z}\right)_{F}, \tag{3.11}$$

where the subscripts PE, KE, F refer to Potential Energy, Kinetic Energy, and Friction respectively. Usually, the individual correlations are valid only for certain types of flow regimes and well inclinations. The Gray Correlation is used for tubing flow calculations in this thesis and will be described in more detail.

3.6 The Gray Correlation

The Gray Correlation was developed specifically for wet gas wells and is commonly used for gas wells producing free water and/or condensate with the gas (Economides et al., 2013). The correlation is developed originally for vertical wells. Recent experiments from the University of Tulsa have modified the Gray correlation to accurately model inclination effects (Oyewole, 2015). The correlation is used to empirically calculate the potential energy gradient and the frictional pressure gradient. The terms in the mechanical energy balance in Eq. 3.11 is defined by Gray (API, 1978) as

$$\left(\frac{\partial p}{\partial z}\right)_{PE} = \frac{g}{g_c}\left[\epsilon\rho_g + (1-\epsilon)\rho_l\right] = \frac{g}{g_c}\bar{\rho} \tag{3.12}$$

$$\left(\frac{\partial p}{\partial z}\right)_F = \frac{f_f G^2}{2 g_c d \rho_m} \tag{3.13}$$

$$\left(\frac{\partial p}{\partial z}\right)_{KE} = -\frac{G^2}{g_c} d\left(\frac{1}{\rho_m}\right) \tag{3.14}$$

where ϵ is the empirical in-situ volume fraction of gas, $\bar{\rho}$ is the in-situ volume fraction of gas weighted density, G is the mass velocity ($\rho_m v_m$), f_f is the Fanning friction factor, and ρ_m is the input fraction weighted density. The input fraction weighted density is simply

$$\rho_m = \lambda_l \rho_l + (1 - \lambda_l)\rho_g \tag{3.15}$$

where

$$\lambda_l = \frac{v_{sl}}{v_{sl} + v_g}. \tag{3.16}$$

In the Gray correlation liquid densities were taken to be independent of pressure and temperature. Another important assumption is that there is no solution condensate in the gas, such that $r_s = 0$. This means that the condensate flow rate, measured in surface volumes, is constant. Condensate flow rate will only be a function of pressure in the tubing through the oil formation volume factor B_o. From dimensional analysis and laboratory tests, four dimensionless parameters were found to influence holdup

$$N_v = \frac{\rho_m^2 v_{sm}^4}{g\tau(\rho_l - \rho_g)} \tag{3.17}$$

$$N_D = \frac{g(\rho_l - \rho_g)d^2}{\tau} \tag{3.18}$$

$$R = \frac{v_{sl}}{v_{sg}} \tag{3.19}$$

$$B = 0.814\left[1 - 0.0554 ln\left(1 + \frac{730R}{R+1}\right)\right] \tag{3.20}$$

Using these four parameters the in-situ volume fraction of gas, ϵ, is calculated using the equation

$$\epsilon = \frac{1 - Exp\left(-2.314\left[N_v\left(1 + \frac{205}{N_D}\right)\right]^B\right)}{R+1}. \tag{3.21}$$

The pseudo interfacial tension of the mixture, τ_m, is calculated using the equations

$$\tau_o = 0.044 - 1.3 \times 10^{-4}(T - 460)\left(\frac{p_d - p}{p_d - 2120}\right)^{2.5} \tag{3.22}$$

$$\tau_w = (2.115 - ln(p))\left[0.174 - 2.09 \times 10^{-4}(T - 460)\right] \tag{3.23}$$

$$\tau_m = \frac{q_o\tau_o + 0.617 q_w \tau_w}{q_o + 0.617 q_w}. \tag{3.24}$$

As the flow regime in the Gray correlation is assumed to be annular flow, a pseudo wall roughness r is used to obtain a two-phase friction factor. The pseudo wall roughness is given by the function

$$r = \begin{cases} r' = 28.5\frac{\tau}{\rho_m v_m^2} & R \geq 0.007 \\ r_g + R\frac{r' - r_g}{0.007} & R < 0.007 \end{cases} \tag{3.25}$$

under the limitation that $r \geq 2.77 \times 10^{-5}$ ft $= 3.324 \times 10^{-4}$ in (Oudeman, 2007).

It is then apparent that in the case of dry gas that $R = 0$, and the pseudo wall roughness is equal to r_g, which is simply the absolute roughness of the pipe. The typical value of absolute roughness is 0.0006 in, while Gray recommends using a value of 0.00094 in. Reynold's number is assumed to be equal to 10^7 (API, 1978). The friction factor is calculated using standard methods, for example the Chen equation.

3.6.1 Modification of the Gravitational Component

A limitation of the Gray Correlation is that of low flow rates. Through the four dimensionless parameters, the in-situ volume fraction of gas, ϵ, approaches zero when gas rates approach zero. This further means that the gravitational component approaches the liquid density at low rates. This method grossly overestimates the pressure drop in gas wells, and also means that the original Gray Correlation cannot be used to calculate static pressure.

This problem was resolved by altering the average density used to calculate the gravitational component. Rather than using the in-situ volume fraction of gas weighted density, $\bar{\rho}$, the input fraction weighted density, ρ_m is used instead. The gravitational pressure drop component is

[1] (API, 1978) has a spelling error here, that is resolved by (Oudeman, 2007). In the API source the denominator is 0.0007 rather than 0.007

then

$$\left(\frac{\partial p}{\partial z}\right)_{PE} = \frac{g}{g_c}\rho_m \tag{3.26}$$

Further on this is referred to as *The Modified Gray Correlation*. This modification results in more physically sound results at low rates. The effect is shown in **Fig. 3.4**.

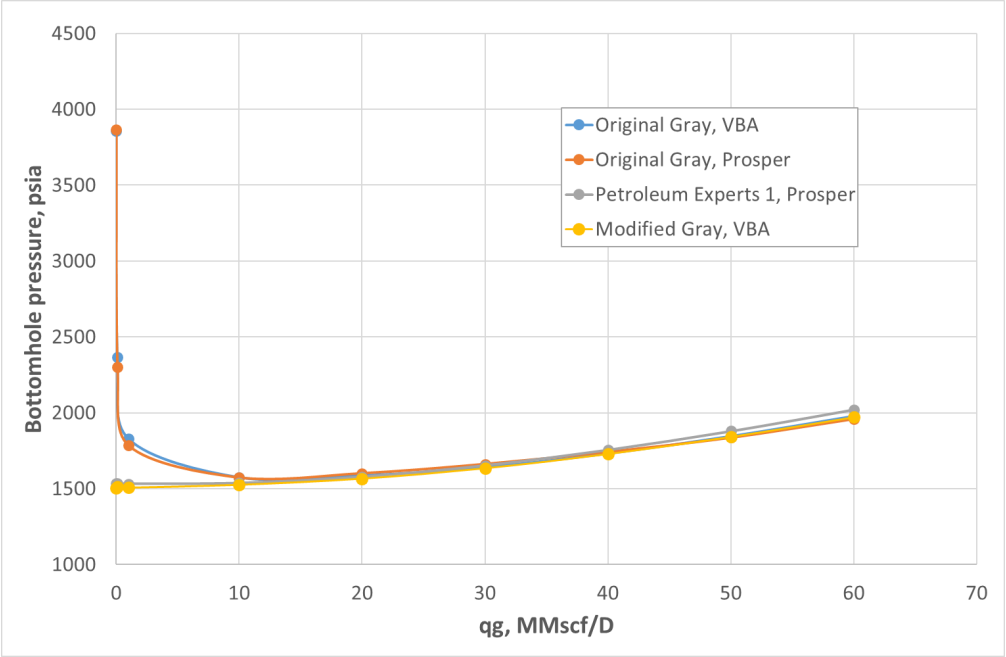

Figure 3.4: Relationship between bottomhole pressure and rate for different tubing flow correlations. In this example p_t=1200 psia and CGR=40 STB/MMscf. BHP increases massively at low rates for the Original Gray correlation. In the Modified Gray the low rate behavior closely resembles behavior of the *Petroleum Experts 1 Correlation*, a common tubing correlation used in Prosper.

A note on units

For Eq. 3.12 - 3.14, the output of the pressure gradient is lb_f/ft^3.

For Eq. 3.17 - 3.21, the output is dimensionless. Input density is in lb_m/ft^3, velocity is in ft/s, interfacial tension in lb_m/s^2, diameter in ft, gravitational acceleration is 32.17 ft-lb_m/lb_f-s^2.

For Eq. 3.22 - 3.24, the output is lb_m/s^2. The input temperature is in °R while the input pressure is in lb_f/ft^2. To convert from lb_m/s^2 to dynes/cm multiply with 454.

For Eq. 3.25, the wall roughness has output inches. The input interfacial tension is in lb_m/s^2, the density in lb_m/ft^3 and the velocity is in ft/s.

Chapter 4

Steady-State Simulation Model Description

This chapter describes the methodology behind developing the steady-state simulation model. The simulation model is a combination of two separate models; one model describing reservoir behavior and one model describing tubing behavior. The two models are coupled to be able to simulate changes throughout the entirety of the system.

4.1 Simulation Program Selection

The simulation model is built in Microsoft Excel using VBA (Virtual Basic for Applications). Microsoft Excel is an extremely versatile program that is used across all industries, from finance to engineering. VBA is an implementation of Microsoft's event-driven programming language Visual Basic 6, allowing for easy access to programmed functions through the standard Microsoft Excel interface (Wikipedia, 2017).
Excel VBA was chosen as the simulation software due to several reasons:

- The syntax is simple, and code written in VBA will be understandable to most people with basic programming knowledge.
- VBA functions can be accessed through the standard Microsoft Excel interface, allowing for easy access and testing
- The computational requirements in the model were anticipated to be low.

- I had some previous experience with VBA, and was interested in becoming more proficient using Excel.
- Excel allows for simple and instantaneous visualization of calculated data.

It was also an option to do the programming in Matlab, or it could be possible to use commerical simulators. Use of commercial simulators might be a good solution, but will definitely not give the same understanding as one acquires from programming the functions from scratch.
Due to the reasons listed above Excel was chosen.

4.2 Model Concept

The concept of the simulation model was to incorporate a steady-state reservoir model and a tubing model that would capture the effects of gas condensate production on the entirety of the system. The reservoir model and the tubing model were built independently using Excel VBA, then set up in an Excel spreadsheet in such a way that a parameter alteration done on one part of the model would change the behavior of the other part of the model. A simple schematic of the model is shown in **Fig. 4.1**.

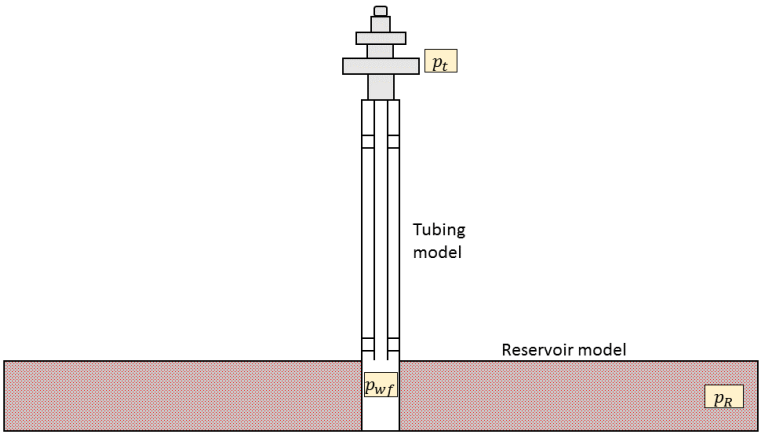

Figure 4.1: Schematic of the simulation model

4.3 Steady-State Reservoir Model

The purpose of the reservoir model is to calculate the production rate for a given p_{wf}. Knowing the production rate is essential in this case because the pressure drop in the tubing is a function both of rate and p_{wf}.

4.3.1 Dry Gas Rate

In the case of single phase dry gas, the production rate is calculated using Eq. (2.8). By rearranging the equation and solving for q, we obtain

$$q = \frac{-A_{bh} + \sqrt{A_{bh}^2 + 4B_{bh}\Delta p_p}}{2B_{bh}}. \tag{4.1}$$

A_{bh} and B_{bh} are constants that depend on the reservoir parameters. Δp_p is solved using numerical integration. Pseudopressure calculation requires pressure dependency of z and μ_g. Gas z-factor is calculated using the *Hall and Yarborough* correlation, and gas viscosity is calculated using the *Lee-Gonzalez* correlation. Pseudocritical properties are calculated using the *Sutton* correlation, with the *Aziz* correction for gas impurities.

Validation of Dry Gas Functions

The functions used to calculate dry gas rate are validated against examples from two renowned textbooks; *Petroleum Production Systems* (Economides et al., 2013) and *Gas Reservoir Engineering* (Lee and Wattenbarger, 1996). The comparisons can be seen in **Fig. 4.2** and **Fig. 4.3**.

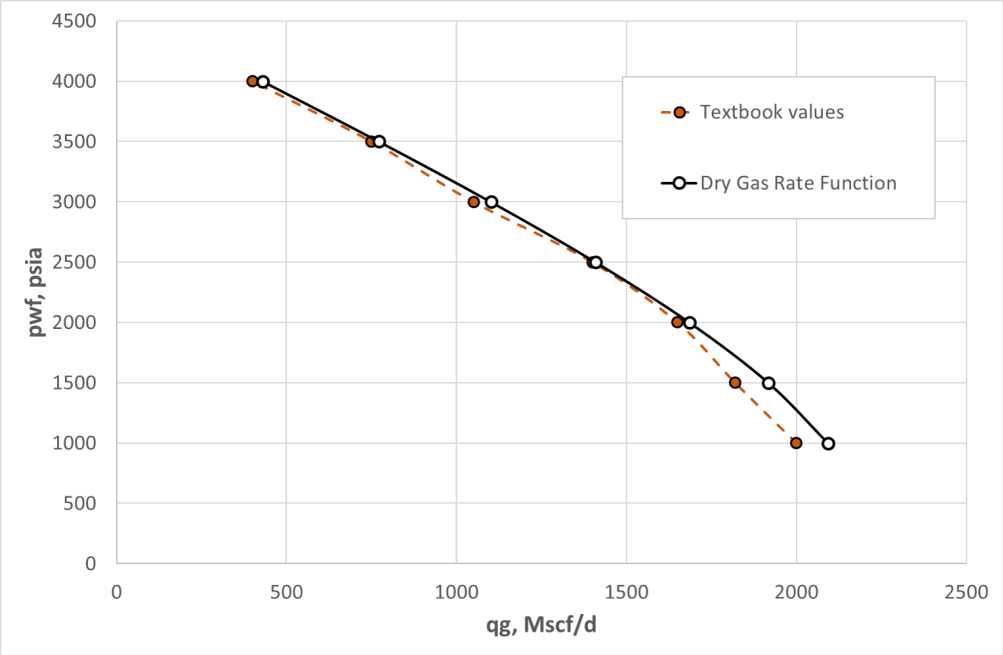

Figure 4.2: Example 4.6 in *Petroleum Production Systems* (Economides et al., 2013). The textbook values were calculated using pressure-squared, and the "Dry Gas Rate" function uses gas pseudopressure. This explains the discrepancy at large drawdowns.

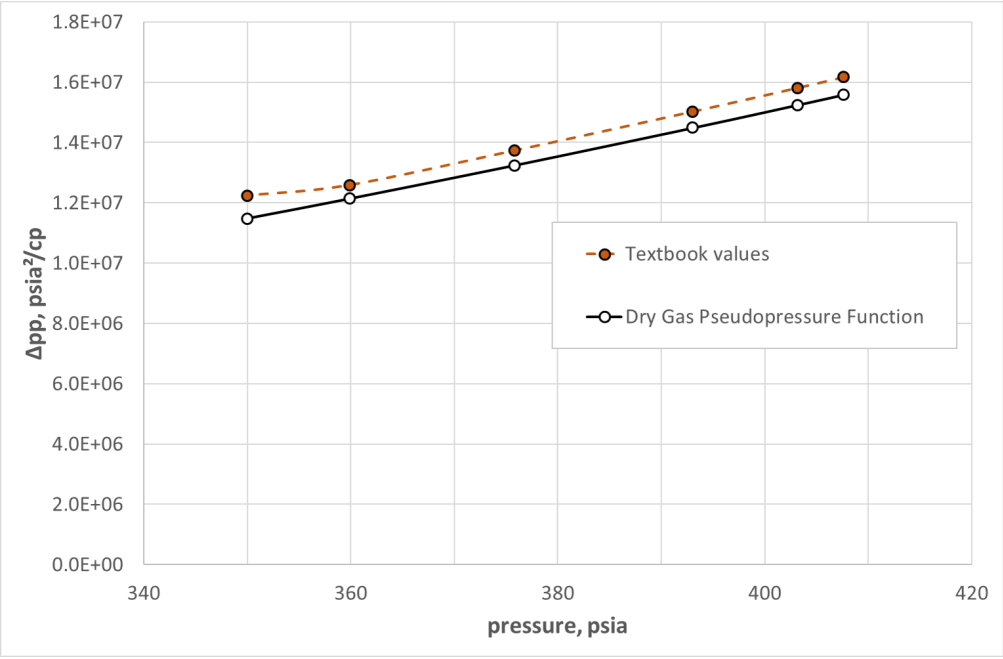

Figure 4.3: Example 7.1 in *Gas Reservoir Engineering* (Lee and Wattenbarger, 1996). The maximum error in this interval is 4%. Discrepancies may be explained by the use of different correlations for viscosity and z-factor.

4.3.2 Gas Condensate Rate

The gas condensate rate equation in terms of black-oil PVT is given as (Fevang and Whitson, 1995)

$$q_g = \alpha \int_{p_{wf}}^{p_R} \left(\frac{k_{rg}}{B_{gd}\mu_g} + \frac{k_{ro}}{B_o\mu_o}R_s\right)dp, \tag{4.2}$$

where

$$\alpha = \frac{kh}{141.2 \times 10^3 (ln(r_e/r_w) - 0.75 + s)} \tag{4.3}$$

for field units and gas rate in MMscf/D.

Black-oil PVT functions were created using known PVT data for two different gas condensates, "Lean fluid" and "Rich fluid". Fluid properties are given in Table 4.1.

Table 4.1: Fluid data for the fluids used to calculate the gas condensate pseudopressure integral. Separator conditions (p, T): Stage 1 (375psia, 108°F), Stage 2 (14.7psia, 60°F). Table modified from (Fevang and Whitson, 1995). Note that 'Initial Reservoir Pressure' does not refer to the reservoir pressure used in any simulations.

	Rich fluid	Lean fluid
Initial Reservoir Pressure, psia	6500	5500
Initial Reservoir Temperature, °R	266	315
Dewpoint Pressure, psia	5900	5400
Maximum CVD Liquid Dropout, %	24	2
Initial Solution OGR rs, STB/MMscf	175	45
STO API Gravity, °API	55	45

Lab data from a Constant Composition Expansion (CCE) test and a Constant Volume Depletion (CVD) test were available for both fluids. This data was used to create both saturated and undersaturated pressure dependent functions of the black-oil variables. The functions were utilized according to the calculation method described in Section 3.3. Two sets of functions were made; one set for the lean fluid and one set for the rich fluid.

Validation of Gas Condensate Functions

Calculations of gas condensate rate are more complicated and not as common as dry gas rate calculation. This made quality control more challenging. The chosen approach was to compare pressure behavior of gas condensate rates with dry gas rates. The expectation was that, for a

given bottomhole flowing pressure, the richer fluid would see the largest drop in flow rate. Estimating the difference is difficult, but it was expected that the rates were within the same order of magnitude. As shown in Fig. 2.1, the deliverability of a heavier gas can be significantly lower than the deliverability for a lean gas due to the shape of the pseudopressure function. Using the two-phase pseudopressure function created in Excel VBA, this effect is shown in **Fig. 4.4**. In this figure the gas relative permeability reduction from condensate dropout is ignored by forcing $k_{rg} = 1.0$. This lets the calculation results compare to those of dry gas. The expected deliverabil-

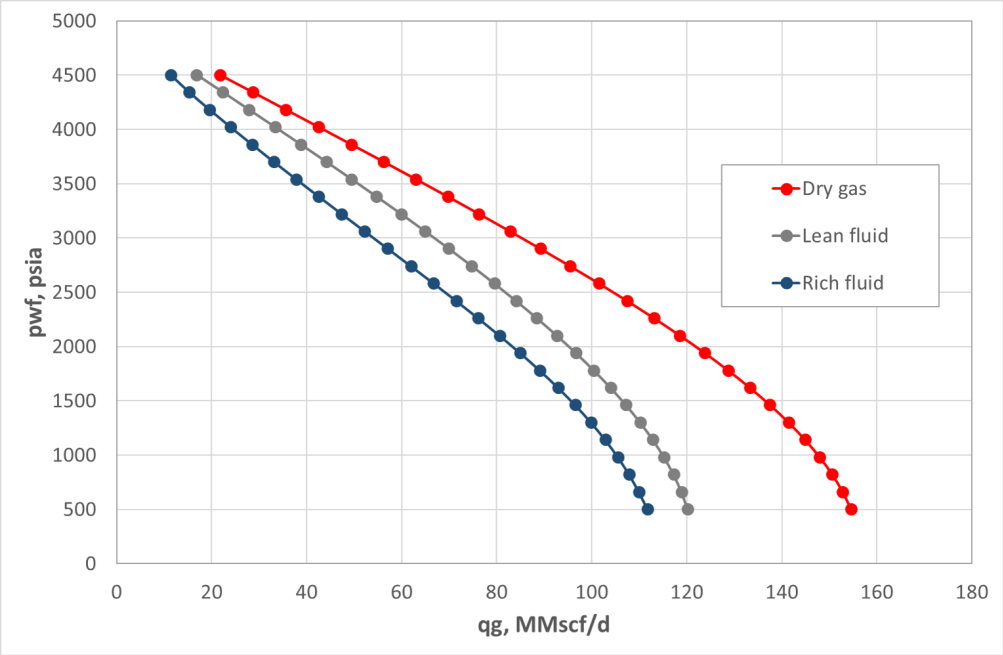

Figure 4.4: Reservoir deliverability ignoring two-phase (condensate) flow, where gas PVT property differences in the three fluid systems yield the three curves.

ity loss from condensate blockage is very high, especially when the reservoir pressure is below the dewpoint. This is shown in **Fig. 4.5**, where gas rate is drastically reduced in the case where relative permeability is pressure dependent. This is an extreme case as the reservoir pressure is below the dewpoint; the difference would not be as large if the reservoir pressure was higher. In the case of the lean fluid the rate is approximately decreased by a factor of three. This is expected from comparing the area under the $(k_{rg}/\mu_g B_g)$ curves in Fig. 3.3. The relative permeability loss for the rich fluid is even higher than for the lean fluid.

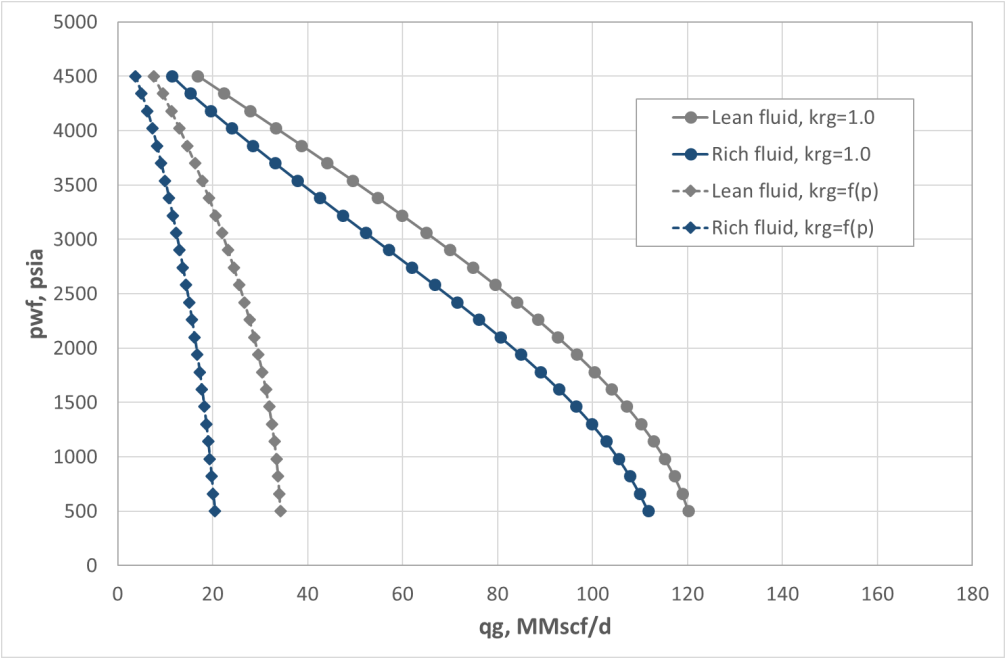

Figure 4.5: Reservoir deliverability loss due to condensate blockage with gas relative permeability decrease predicted by the Fevang & Whitson model.

4.4 Tubing Model

The purpose of the tubing model is to

1. Calculate the wellhead flowing tubing pressure, p_t, for a combination of flow rate and flowing bottomhole pressure, p_{wf}.

2. Calculate the flowing bottomhole pressure, p_{wf}, for a combination of flow rate and wellhead flowing tubing pressure, p_t.

The relationship between these three codependent parameters was modeled using the Gray Correlation. Using Excel VBA, Purpose (1) and (2) were solved using two different programs. For a given combination of flowing pressure and rate, the programs calculate the required pressure by dividing the wellbore into a number of segments depthwise. By starting at either the top or the bottom of the tubing, a local pressure gradient is calculated. The pressure gradient is used to calculate the pressure at the next depth segment in a step-wise process. This process is continued until the final depth is reached.

Validation of the Gray Correlation

The implemented tubing model was validated in two different ways

1. Comparison of results to the Fetkovich approach for flow of single-phase gas
2. Comparison of results from Prosper for two-phase flow

Verification of the Gray Correlation for single-phase gas is shown in **Fig. 4.6**. The maximum difference throughout this interval is 3%, which is at an extremely low tubing pressure. A flowing tubing pressure of 50 psia is likely pushing the validity of either model.
Comparison with Prosper for varying CGR is shown in **Table 4.2 - 4.4**. The maximum difference seen here is 4%. Calculations with multiphase flow have larger potential for difference than for single phase due to the complexity of phase behavior, heat loss modeling, and so forth. In the VBA tubing model the temperature increase is assumed to be linear with depth, while Prosper utilizes more sofisticated models to calculate temperature in the tubing.

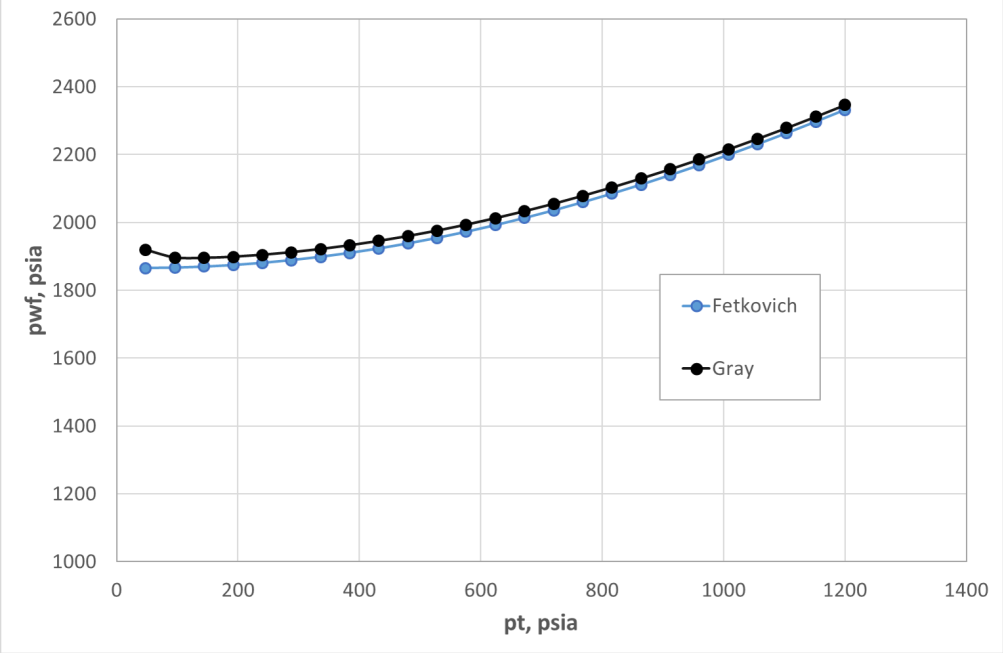

Figure 4.6: Comparison of results from calculations using the Fetkovich method and the Gray Correlation for dry gas (CGR=0 STB/MMscf). q=25 MMscf/d in this example.

Table 4.2: CGR = 40 STB/MMscf

q_g	p_t	T_t	p_{wf} *Prosper*	p_{wf} *VBA*	Difference
MMscf/d	psia	°F	psia	psia	
5	1200	129	1622	1598	1 %
10	1200	140	1753	1713	2 %
15	1201	149	1934	1926	0 %
20	1201	156	2156	2197	2 %
25	1202	161	2444	2508	3 %
30	1203	166	2758	2845	3 %

Table 4.3: CGR = 70 STB/MMscf

q_g	p_t	T_t	p_{wf} *Prosper*	p_{wf} *VBA*	Difference
MMscf/d	psia	°F	psia	psia	
5	1200	131	1688	1648	2 %
10	1200	143	1836	1784	3 %
15	1201	152	2039	2029	0 %
20	1201	159	2304	2338	1 %
25	1202	164	2630	2689	2 %
30	1203	169	2984	3073	3 %

Table 4.4: CGR = 100 STB/MMscf

q_g	p_t	T_t	p_{wf} *Prosper*	p_{wf} *VBA*	Difference
MMscf/d	psia	°F	psia	psia	
5	1200	132	1760	1698	4 %
10	1200	145	1924	1856	4 %
15	1201	155	2150	2133	1 %
20	1201	162	2460	2480	1 %
25	1202	167	2825	2874	2 %
30	1203	171	3219	3303	3 %

4.5 Coupled Model

The coupled model incorporates both the tubing model and the reservoir models into a single spreadsheet. The spreadsheet works in such a way that if any reservoir characteristics are changed, the response in flowing tubing pressure is seen instantly. Conversely, a change in the diameter of the tubing would alter the bottomhole pressure, and hence the production rate. The working functionality is shown below.

Input:

- Reservoir parameters: $k, h, p_R, T_R, r_e, r_w, s, S_{wi}$
- Tubing parameters: D, T_t, L
- Fluid data: $r_p, \gamma_g, \gamma_o, p_D$

Functionality:

1. Select a reservoir fluid system: Dry Gas, Lean Gas Condensate, or Rich Gas Condensate.
2. Set the range of p_{wf}. The specified reservoir model determines the production rate, q_g, based on reservoir parameters, fluid data, and the wellbore flowing pressure.
3. The tubing model determines the flowing tubing pressure, p_t, based on tubing parameters, fluid data, wellbore flowing pressure, and production rate.

Chapter 5

Results & Discussions

This chapter describes the results that were generated from the steady-state Excel VBA model. In total, six backpressure curves are presented for each of the three fluid systems. Results from both a "low" and a "high" pressure case are presented. This includes two reservoir deliverability curves, tubing friction curves, and wellhead flowing curves for each fluid. Universal parameters used in the calculations are given in **Table 5.1**.

Table 5.1: Parameters used in simulation of backpressure curves

Parameter	Value
Reservoir pressure p_R, psia	2500 ("low"), 8000 ("high")
Reservoir temperature T_R, °F	200
Absolute permeability k, md	40
Relative permeability @ Swi, -	1.0
Reservoir height h, ft	10
Irreducible water saturation S_{wi}, %	25
Drainage radius r_e, ft	3000
Wellbore radius r_w, ft	0.42
Skin factor s, -	5
Non-Darcy flow constant D, D/MMscf	0
Gas gravity γ_g, -	0.7
Oil gravity γ_o, -	0.8
Well depth L, ft	8000
Tubing temperature T_t, °F	168

5.1 Dry Gas Backpressure Curves

Reservoir backpressure curves (”bottomhole” and ”static” curve) for a low pressure system are shown in **Fig. 5.1**. The solid black lines on top of the data points in the figure are not trendlines, but are lines showing a slope of exactly 1.0 or 2.0. It is apparent that the pressure squared plot is a good fit for a low pressure model. Reservoir backpressure curves for a high pressure system are given in **Fig. 5.2**. The fit is not as good as in the low pressure reservoir since the pseudopressure function is not approximated by pressure squared at higher pressures.

Tubing friction curves for low pressure reservoirs show a near perfect fit to a slope of 2, as shown in **Fig. 5.3**. A slope of 2 is also observed in the high pressure case, as shown in **Fig. 5.4**.

By combining the wellhead static curve and the tubing friction curve as in shown Eq. (2.23), we get a relationship of the pressure drop from the reservoir throughout the tubing. This is shown in **Fig. 5.5**. We see that the slope is approximately equal to 1.0, meaning that the dominant pressure drop is the pressure drop in the reservoir. The wellhead curves for different tubing size almost overlap as the pressure drop in the tubing is insignificant compared to the reservoir pressure drop. Similar behavior is observed in the high pressure case where the reservoir pressure drop dominates the tubing pressure drop. The deviation from slope equal to 1.0 is attributed to deviation from pressure-squared behavior in the reservoir. This is shown in **Fig. 5.6**.

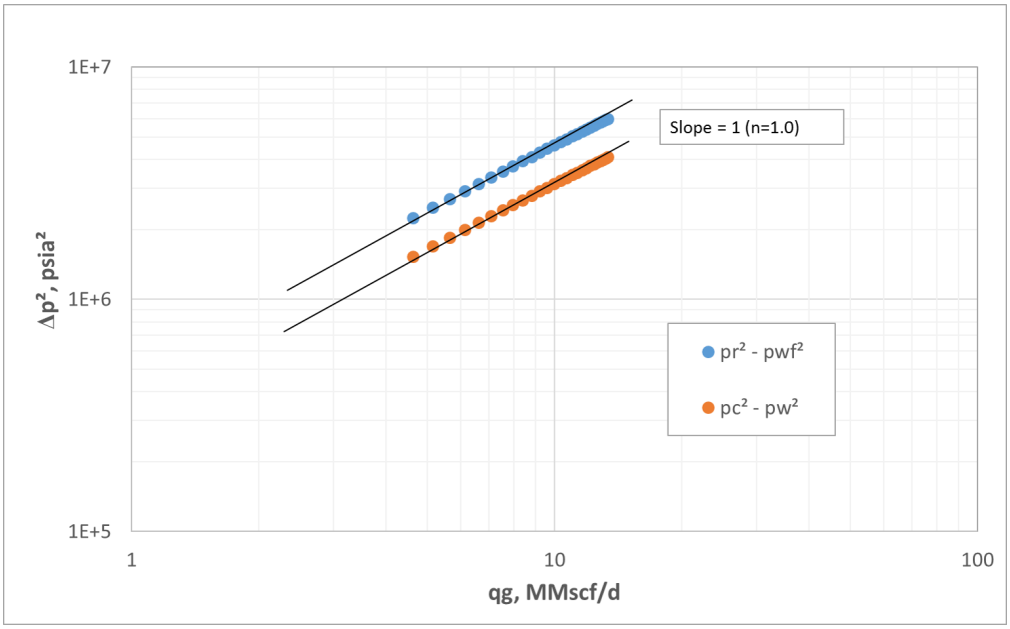

Figure 5.1: Reservoir deliverability curves for a low pressure dry gas reservoir.

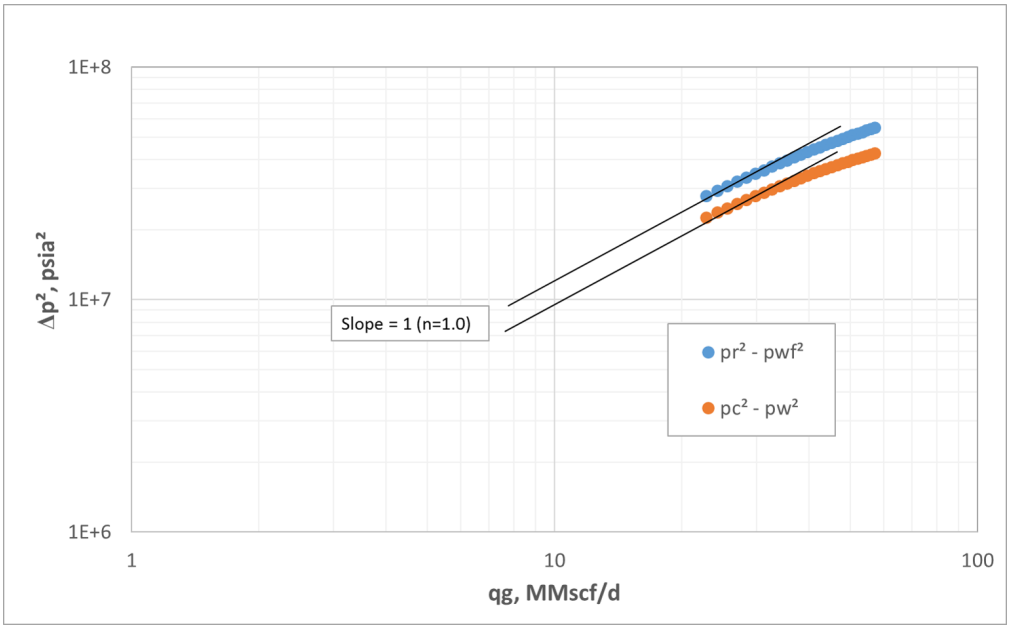

Figure 5.2: Reservoir deliverability curves for a high pressure dry gas reservoir.

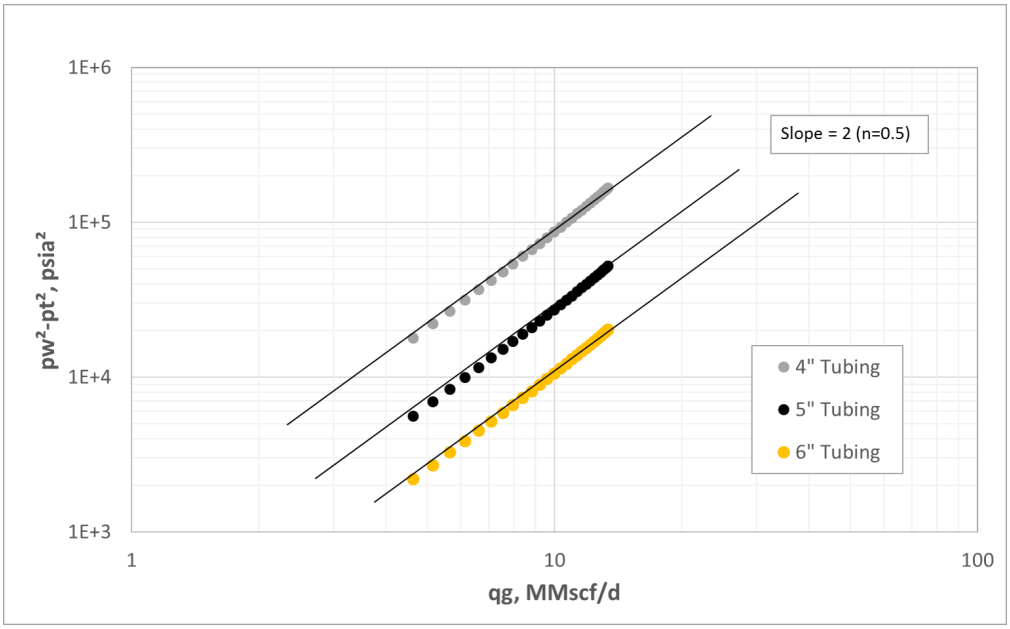

Figure 5.3: Tubing friction curves for a low pressure dry gas reservoir.

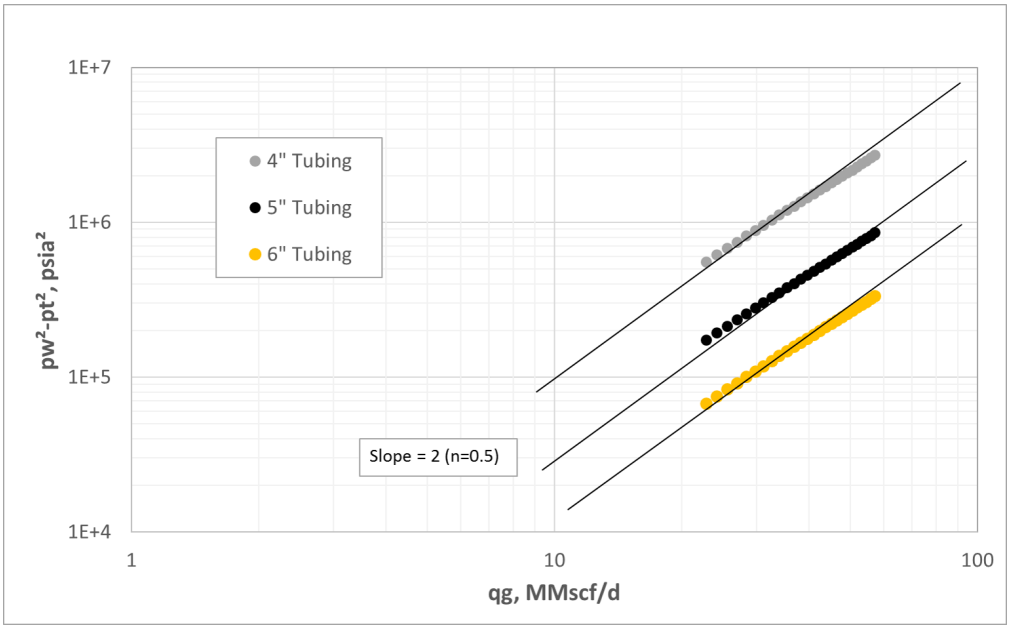

Figure 5.4: Tubing friction curves for a high pressure dry gas reservoir.

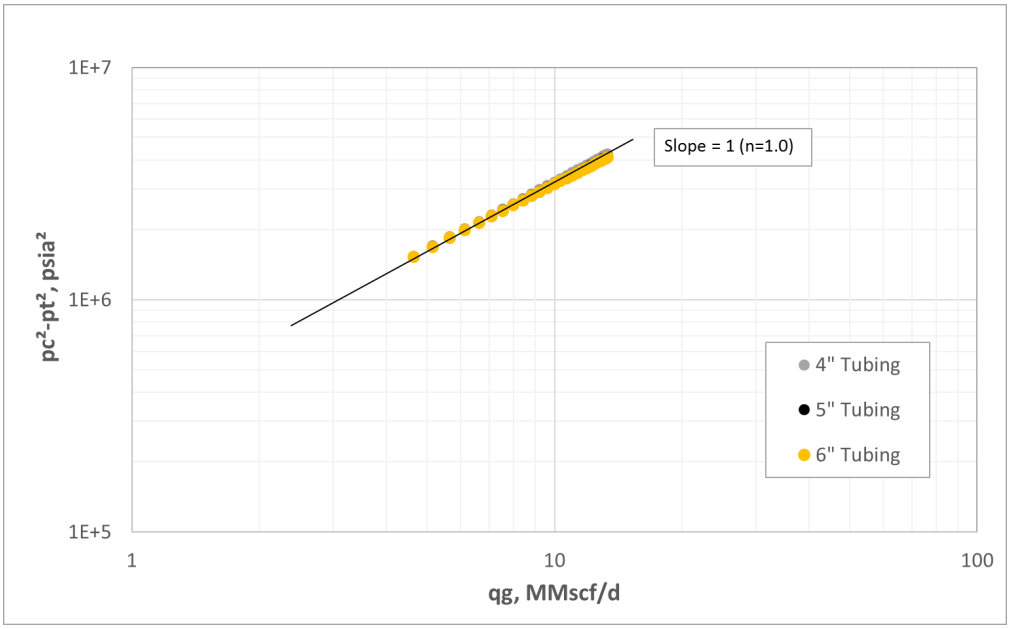

Figure 5.5: Wellhead backpressure curve for a low pressure dry gas reservoir.

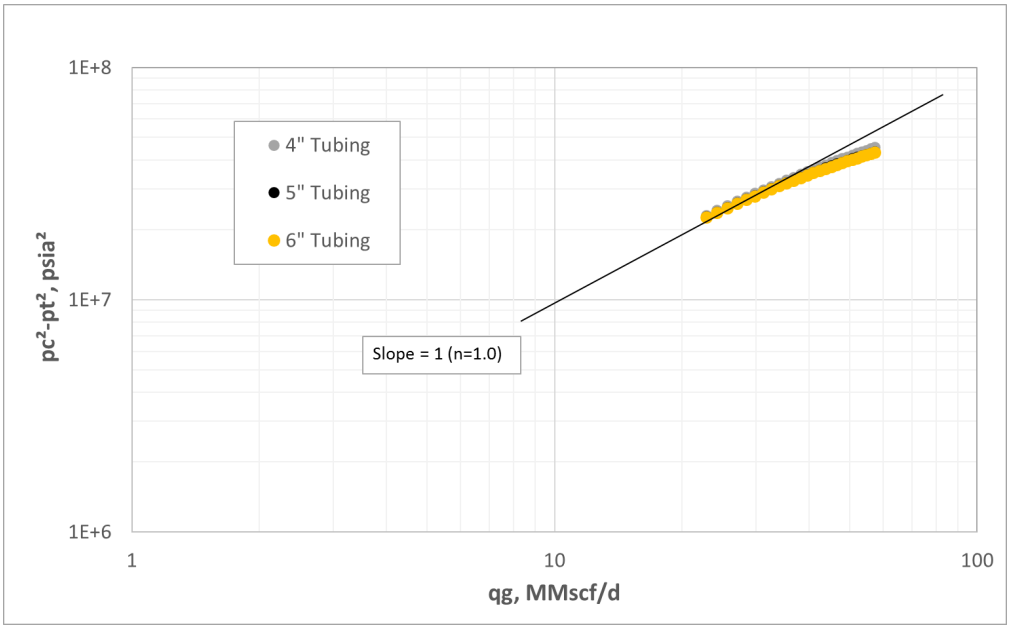

Figure 5.6: Wellhead backpressure curve for a high pressure dry gas reservoir.

5.2 Lean Gas Condensate Backpressure Curves

Reservoir backpressure curves for a low pressure lean gas condensate is shown in **Fig. 5.7**. The curve shows a close fit to a slope of 1.0. Reservoir curves for a high pressure lean gas condensate fits a slope of 1.0 over a certain range of pressures, as shown in **Fig. 5.8**. The slope of the reservoir curves steepen at high drawdowns.

Tubing friction curves for the lean gas condensate follow a slope of 2.0 for the low pressure case, as shown in **Fig. 5.9**. In the high pressure case in **Fig. 5.10** the curve follows a slope of 2.0 initially, but one can observe deviations in the same range as observed in the reservoir curves.

The wellhead backpressure curve for the low pressure case in **Fig. 5.11** follows a slope of 1.0, meaning that the total pressure drop throughout the system is dominated by the pressure drop in the reservoir. The same is observed for the high pressure case in **Fig. 5.12**. The wellhead flowing curve closely resembles the static column curve, and starts to deviate from a slope of 1.0 at high drawdowns.

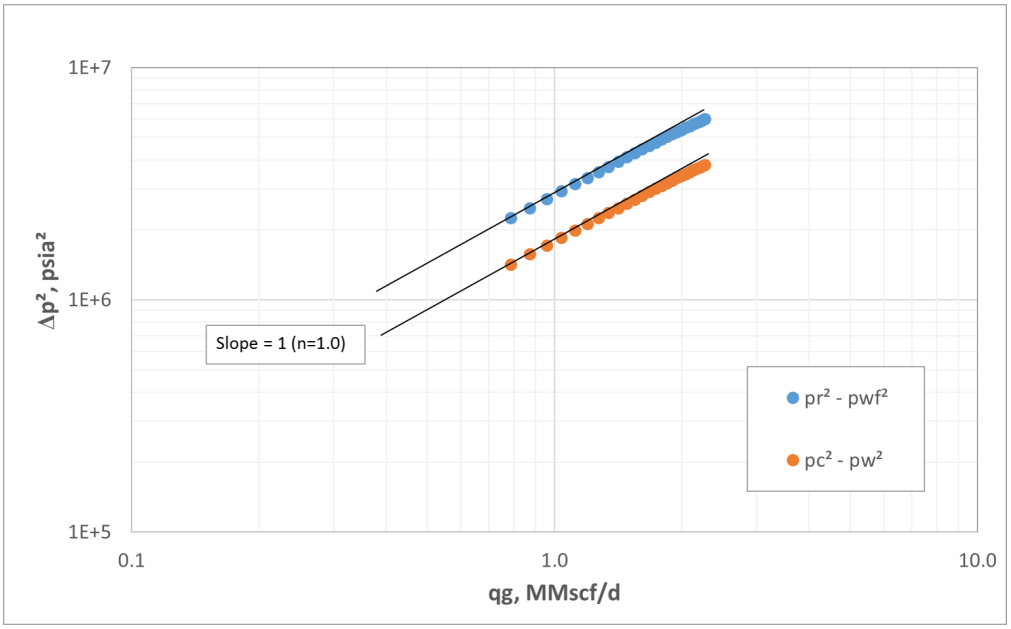

Figure 5.7: Reservoir deliverability curves for a low pressure lean gas condensate reservoir.

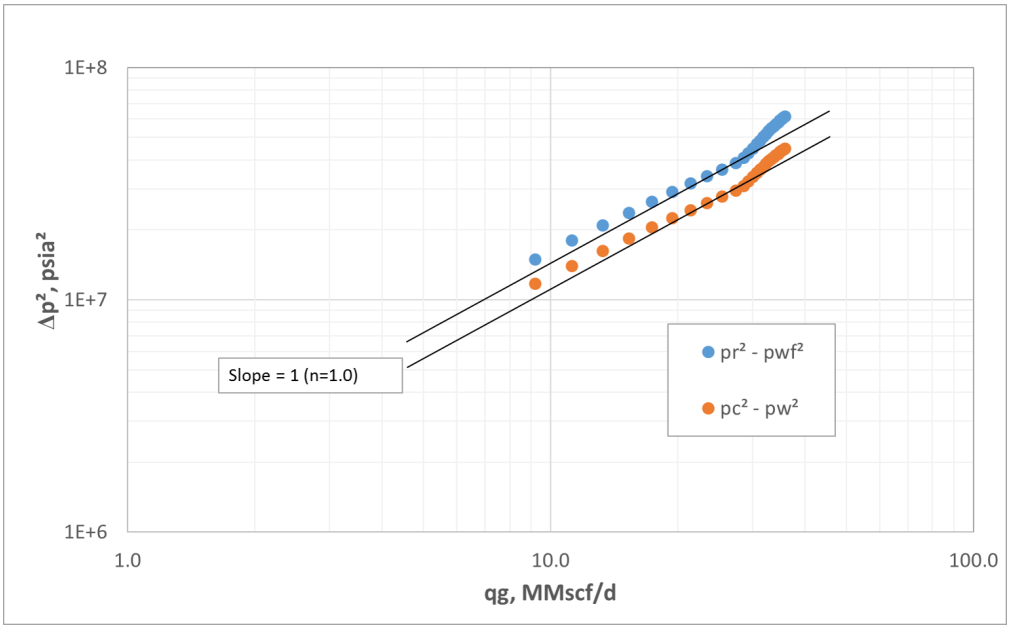

Figure 5.8: Reservoir deliverability curves for a high pressure lean gas condensate reservoir.

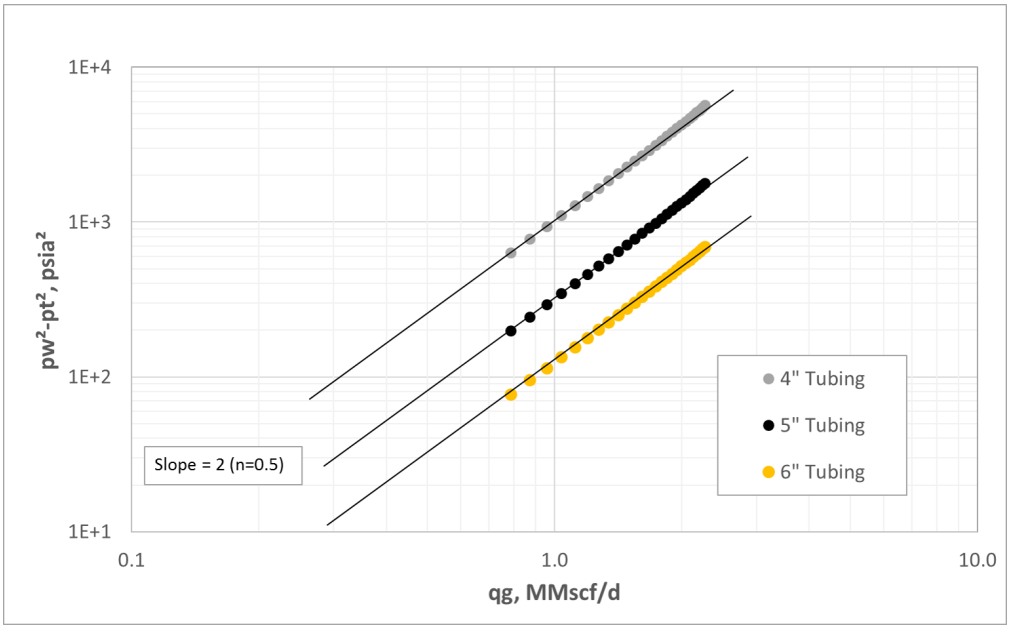

Figure 5.9: Tubing friction curves for a low pressure lean gas condensate reservoir.

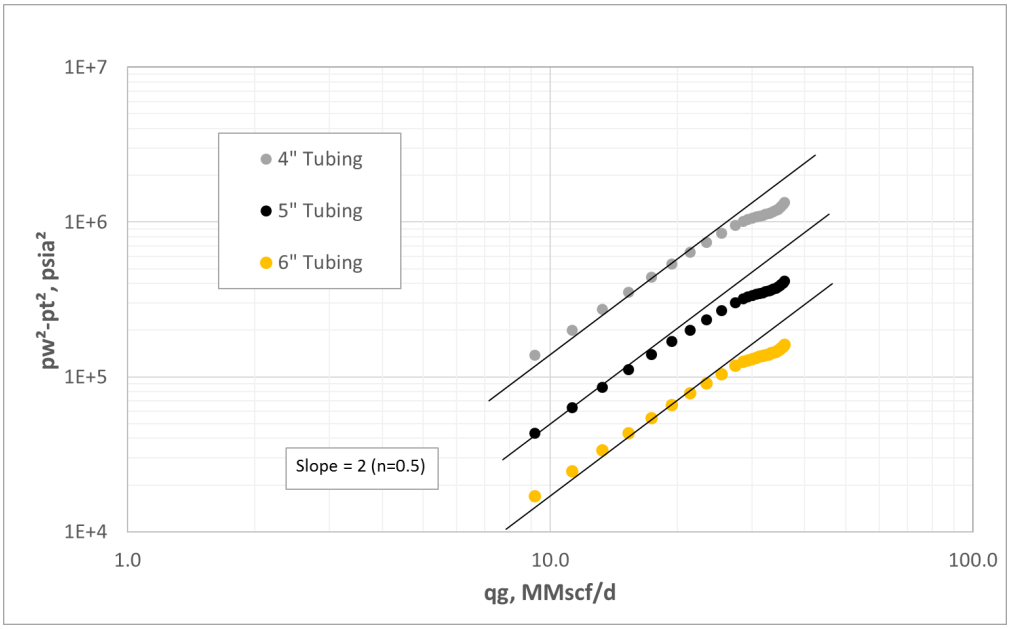

Figure 5.10: Tubing friction curves for a high pressure lean gas condensate reservoir.

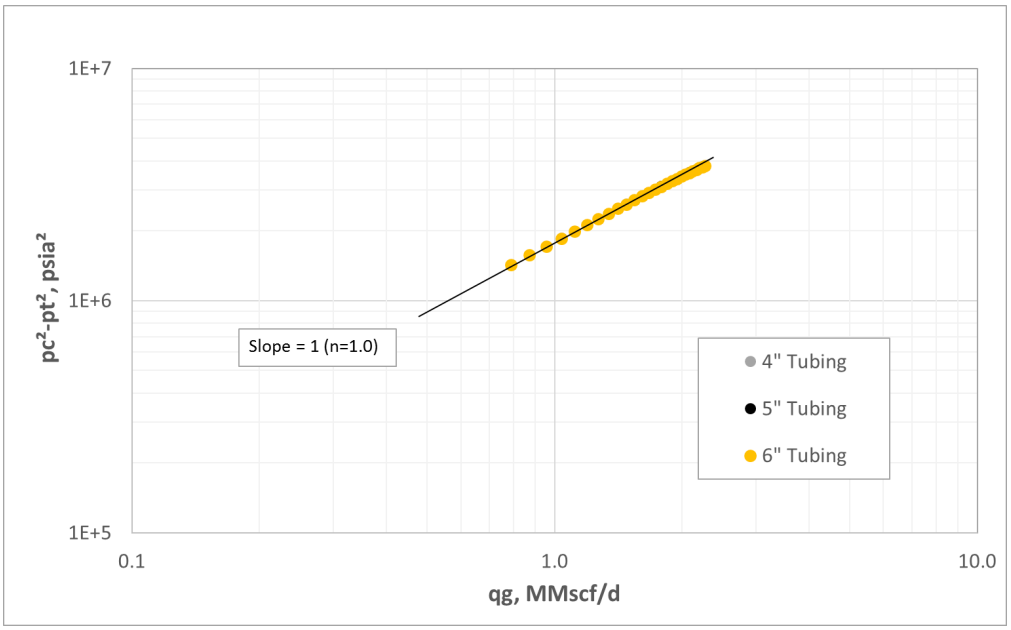

Figure 5.11: Wellhead backpressure curve for a low pressure lean gas condensate reservoir.

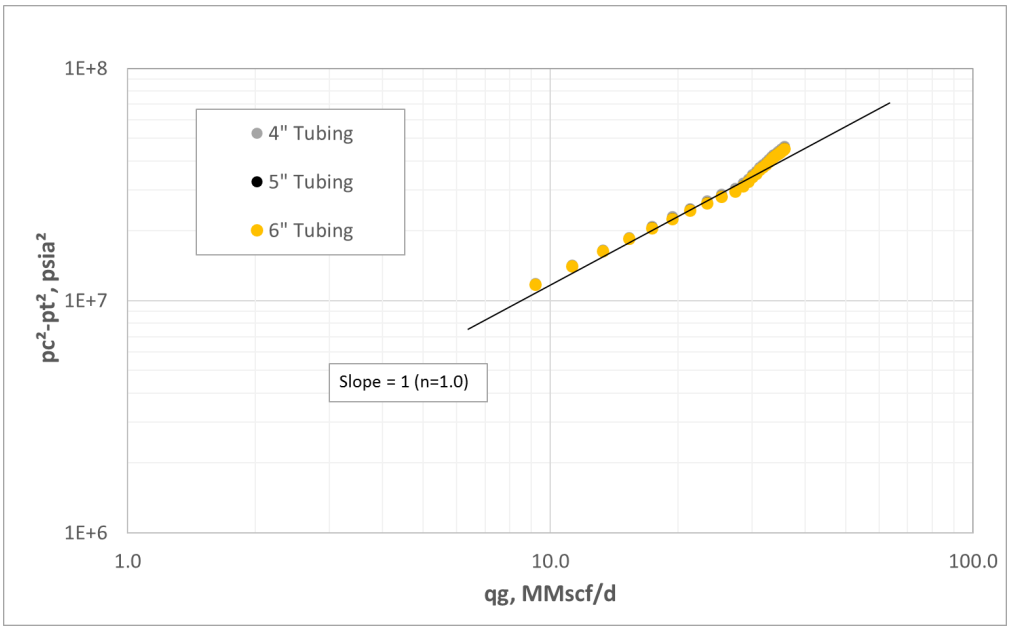

Figure 5.12: Wellhead backpressure curve for a high pressure lean gas condensate reservoir.

5.3 Rich Gas Condensate Backpressure Curves

The results from the Rich Gas Condensate case are similar to the results of the Lean Gas Condensate. Reservoir backpressure curves for a low pressure rich gas condensate is shown in **Fig. 5.13**. The curve shows a close fit to a slope of 1.0. For the high pressure case in **Fig. 5.14** a slope of 1.0 is seen over only a narrow range of pressures. The slope of the reservoir curves steepen at high drawdowns.

Tubing friction curves for the rich gas condensate follow a slope of 2.0 for the low pressure case, as shown in **Fig. 5.15**. In the high pressure case in **Fig. 5.16** the curve follows a slope of 2.0 at low rates, but one can observe deviations in the same range as observed in the reservoir curves. The wellhead backpressure curve for the low pressure case in **Fig. 5.17** follows a slope of 1.0, meaning that the total pressure drop throughout the system is dominated by the pressure drop in the reservoir. The same is observed for the high pressure case in **Fig. 5.18**. The wellhead flowing curve closely resembles the static column curve, and starts to deviate from a slope of 1.0 at high rates.

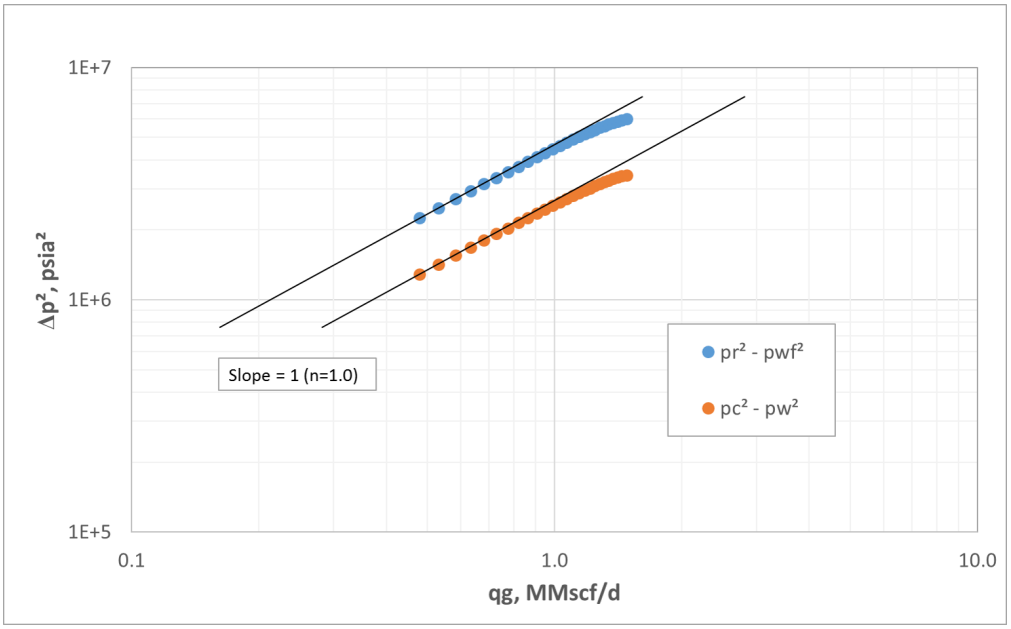

Figure 5.13: Reservoir deliverability curves for a low pressure rich gas condensate reservoir.

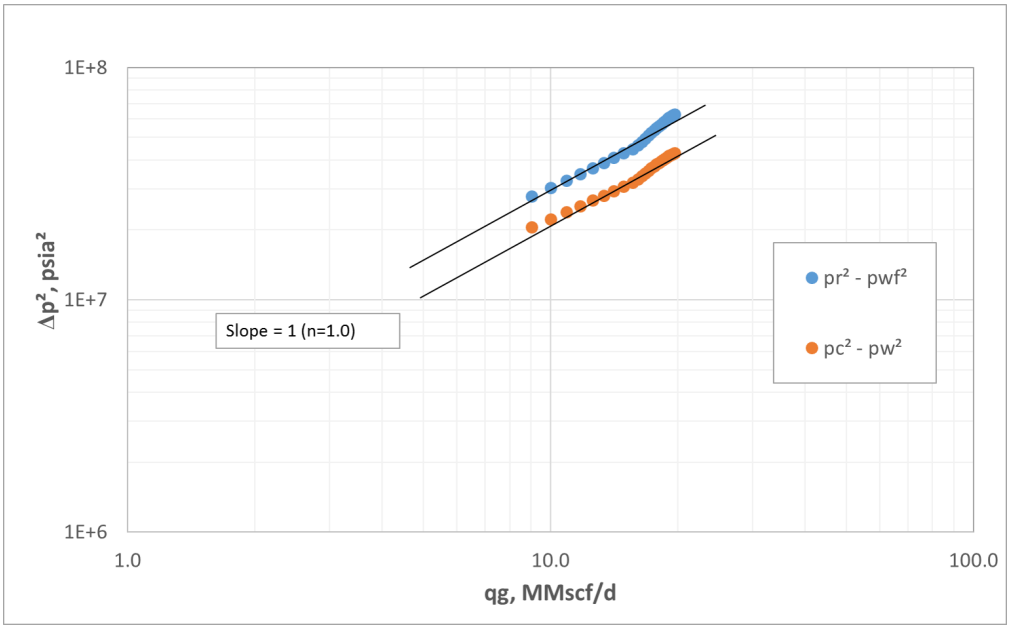

Figure 5.14: Reservoir deliverability curves for a high pressure rich gas condensate reservoir.

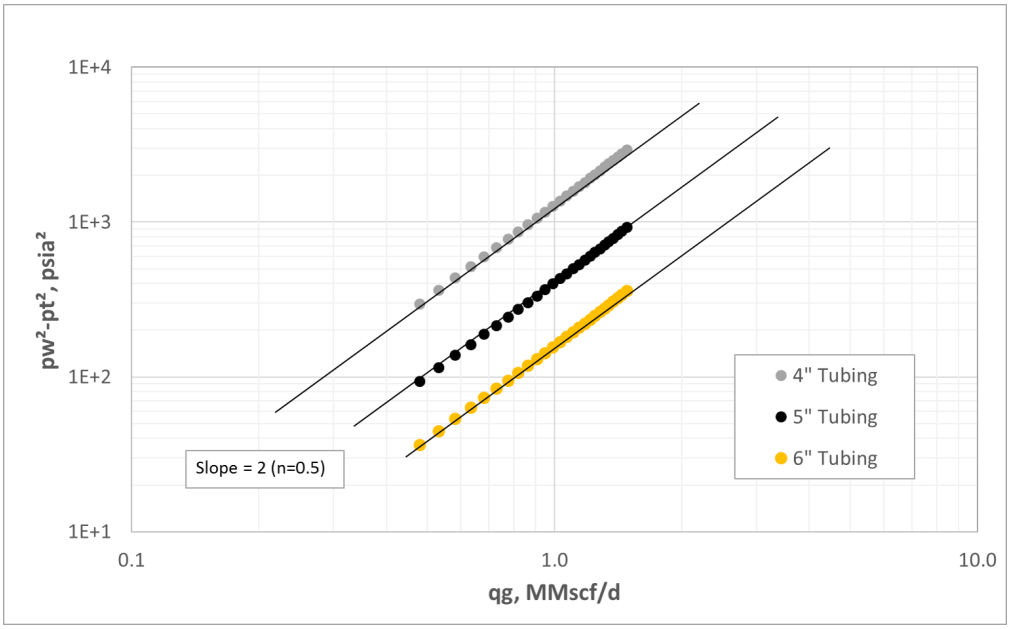

Figure 5.15: Tubing friction curves for a low pressure rich gas condensate reservoir.

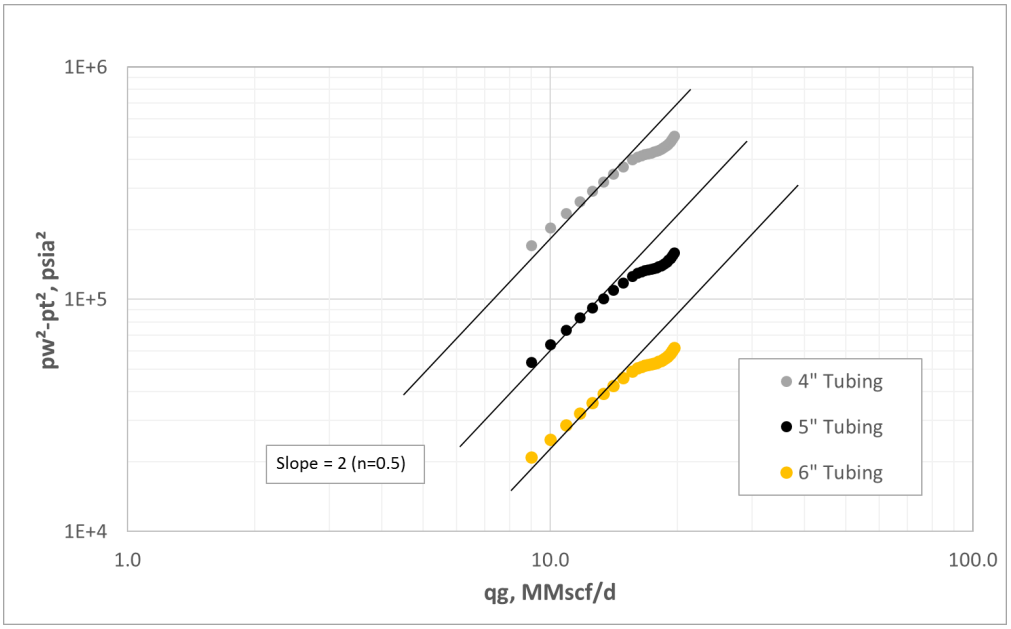

Figure 5.16: Tubing friction curves for a high pressure rich gas condensate reservoir.

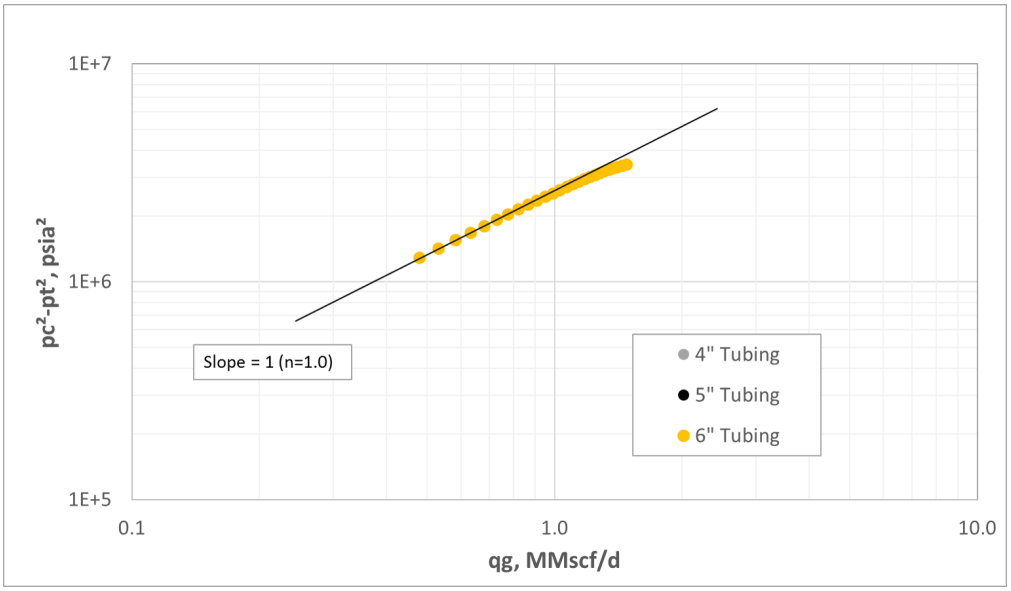

Figure 5.17: Wellhead backpressure curve for a low pressure rich gas condensate reservoir.

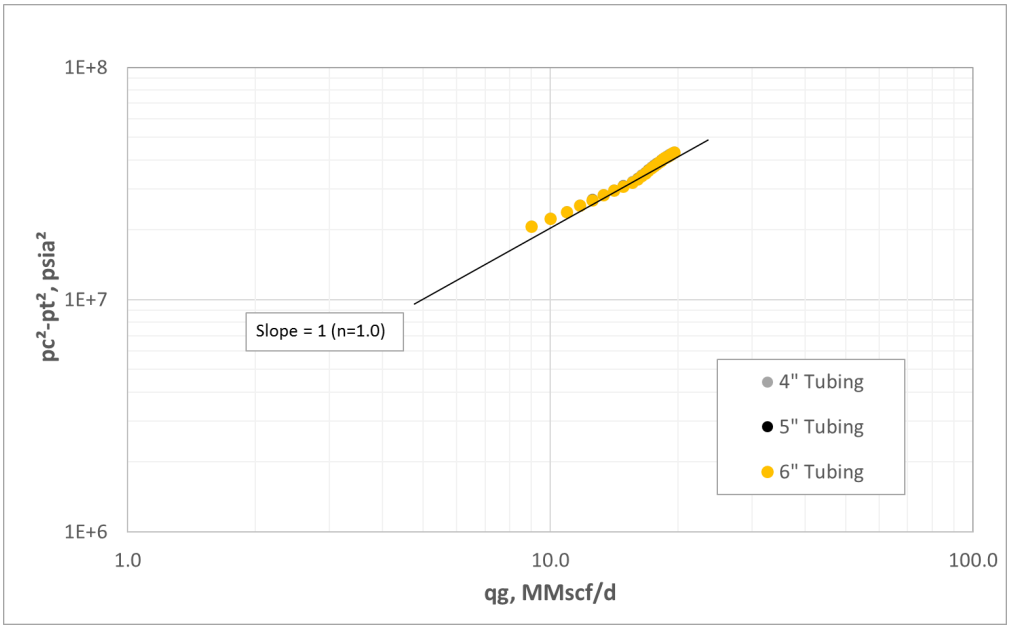

Figure 5.18: Wellhead backpressure curve for a high pressure rich gas condensate reservoir.

5.4 Discussion

5.4.1 Dry Gas Curves

The reservoir curves in the high pressure case show significant deviation from the slope of 1.0. As the pseudopressure function is linear only in the low pressure region, any attempt to model high-pressure behavior using the pressure squared notation will result in deviation from the straight line on traditional backpressure plots. Pressure squred notation is adequate for describing behavior of the low pressure case.

Tubing friction curves are not affected by high-pressure effects, and follow a slope of 2.0 in both the low and the high pressure case.

Wellhead backpressure curves follow a slope of 1.0, meaning that the pressure drop in the production system is dominated by the pressure drop in the reservoir. The tubing sizes used in these simulations are not small enough to inflict any considerable tubing limitation effects. Smaller tubing size would yield a steeper wellhead backpressure curve.

5.4.2 Gas Condensate Curves

Both the lean and the rich gas condensate systems behave similarly with regards to backpressure curves. As expected, the rich gas condensate see lower rates than the lean gas condensate at equal conditions. Deviation behavior from idealized slopes are similar for both fluids, such that the following analysis is applicable to results of both the lean and the rich gas condensates.

Reservoir backpressure curves for the high pressure gas condensates show deviation from the slope of 1.0 at high rates. The explanation for this is the non-linearity of the two-phase pseduopressure function. As shown in Chapter 3.4, the pseudopressure function is not linear when one includes effects of pressure dependent relative permeability. This further means that pressure squared notation is not effective in describing reservoir behavior. Steeper reservoir curves therefore do not necessarily mean that the pressure drop in the reservoir is increasing, but rather that the reservoir model is no longer approximated with the pressure squared notation. Similar observations can be done for the low pressure gas condensate reservoir curves, with slight concave curvature at higher rates. Concave curvature means that a simple pressure squared model

would underestimate the production rate. Conversely, a convex curvature means that a pressure squared model would overestimate the production rate.

The tubing friction curves follow a slope of approximately 2.0 in both the low and the high pressure cases. One can observe a decrease in the slope at an intermediate rate range, but the curve seems to tend towards 2.0 again at the higher rates. This might be attributed to the fact that the Gray Correlation is meant to be used for pressures below the dewpoint. As such, a modification of the term in Eq. (3.22) is required to accomodate cases where $p > p_d$. This is a source of error especially in the pressure region near the dewpoint.

Wellhead backpressure curves closely resemble the static column curve, indicating that the tubing size is not significantly small to inflict any steepening of the curve. Neither of the gas condensate systems are tubing limited.

Chapter 6

Conclusions

- Pressure and rate behavior for dry gas and gas condensates can be incorporated into a coupled well model using Excel VBA. This model can include the effects of steady-state reservoir and tubing flow. The well model can be used to create backpressure curves for dry gas according to the theory by Mike Fetkovich, and can create backpressure curves for gas condensate reservoirs.

- The Gray Correlation is applicable for dry gas and gas condensate wells for a limited range of production rate. For low production rates the correlation will drastically overestimate the pressure drop. This happens because the gravitational pressure component approaches the gravitational pressure component of a liquid column rather than a gas column. By modifying the average density term used to calculate the gravitational pressure component, results from the Gray Correlation are more physically realistic and seem to replicate results from the popular *Petroleum Experts 1* VLP correlation. Without this modification the Gray Correlation should not be used to calculate the static pressure in a gas well.

- Traditional reservoir backpressure curves of Δp^2 vs. q can accurately represent low pressure dry gas, but not high pressure dry gas. This is explained by the shape of pseudopressure function. The pseudopressure function is only linear for pressures lower than approximately 2000 psia.

- Traditional reservoir backpressure curves can not reliabily represent gas condensate systems over a range of production rates. This is due to the non-linearity of the two-phase

pseudopressure functions. Depending on the pressure range, idealized straight line behavior can over- or underestimate the production rate.

- Backpressure curves for lean and rich gas condensate systems show similar behavior for all investigated backpressure curves. In low pressure systems the curves follow slopes similar to dry gas. In high pressure systems lean and rich gas condensates show significant deviations from idealized dry gas behavior.

- Tubing friction backpressure curves for gas condensate flow will have approximately the same slope as for tubing flow of dry gas for both low and high pressures systems.

Chapter 7

Limitations and Future Work

The Gray Correlation, although based on a logical model, was developed for a certain set of tubing, rate, and fluid type. In the original source Gray warned against using the correlation for (1) Flow velocities larger than 50 ft/s, (2) Tubing sizes larger than 3.5 in, (3) Condensate-gas ratios above 50 STB/MMscf, and (4) Water-gas ratios above 5 STB/MMscf (API, 1978). In most of the cases presented in this thesis, one or several of these limiting factors are violated. The magnitude of the error this introduces is not known. Furthermore, the Gray Correlation is not meant to be used for undersaturated mixtures (see Section 5.4). I have also based the accuracy of my Gray Correlation implementation on comparison with results from Prosper. There is of course a possibility that the correlation is not implemented correctly in Prosper. This would mean that my results are untrustworthy.

To further improve the findings of this thesis, one could either implement a more sophisticated VLP correlation, or try coupling a commercial tubing and reservoir simulator. Using commercial simulators does not allow for similar transparency as when programming from scratch, but hopefully allows for more accurate calculations. In addition, using a commercial reservoir simulator allows for analysis of transient behavior rather than using a steady-state model.

Black Oil properties used when calculating two-phase pseudopressure was done using polynomial functions created to fit the provided data sets for the two gas condensate fluids. Most of the BO properties functions required separate functions for saturated and undersaturated properties. Near the dewpoint some of the functions might have been “overfit” due to the behavior in this pressure region.

Acronyms and Nomenclature

Acronyms

AOF Absolute open-flow

BHFP Bottomhole flowing pressure

CCE Constant composition expansion

CGR Condensate/gas ratio

CVD Constant volume depletion

GOR Gas/oil ratio

IPR Inflow performance relationship

J Productivity index

OGR Oil/gas ratio

VLP Vertical lifting performance

Nomenclature

A = drainage area of well, ft^2

A_{bh} = stabilized bottomhole deliverability coefficient for pseudopressure calculations, (psia^2-cp)/(MMscf/D)

A_{wh} = stabilized wellhead deliverability coefficient for pseudopressure calculations, (psia^2-cp)/(MMscf/D)

A'_{wh} = stabilized wellhead deliverability coefficient for pressure squared calculations, psia^2/(MMscf/D)

B = parameter used in the Gray Correlation

B_{bh} = bottomhole deliverability equation coefficient for pseudopressure calculations, (psia^2-

cp)/(MMscf/D)^2

B_{gd} = dry gas FVF, ft^3/scf

B_o = oil FVF, RB/STB

B_{wh} = wellhead deliverability equation coefficient for pseudopressure calculations, (psia^2-cp)/(MMscf/D)^2

B'_{wh} = wellhead deliverability equation coefficient for pressure squared calculations, psia^2/(MMscf/D)^2

c_T = total system compressibility, psia^{-1}

C = stabilized performance coefficient, (MMscf-D/(psia^2-cp)^n) for pseudopressure calculations, or (MMscf-D/psia^{2n}) in terms of pressure squared

C_A = shape factor for well drainage area

C_{tot} = stabilized system performance coefficient for pressure squared calculations, (MMscf-D/psia^{2n})

C_{wh} = stabilized wellhead performance coefficient for pseudopressure, (MMscf-D/(psia^2-cp)^n)

C_{wht} = stabilized wellhead performance coefficient for pressure squared calculations, (MMscf-D/psia^{2n})

d = pipe diameter, in

D = non-Darcy flow constant, D/MMscf

f = friction factor

f_f = Fanning friction factor

f_l = parameter used in the Gray correlation

$F_{\bar{g}g}$ = mole fraction of reservoir gas that remains gas at surface conditions

g = local gravitational acceleration, ft/s^2

g_c = gravitational acceleration constant, 32.2 ft-lb$_m$/lb$_f$-s^2

G = mass velocity, lb$_m$/ft^2-s

G_k = parameter used to estimate relative oil volume for Region 2 Calculation

h = height, ft

k_g = gas effective permeability, md

k_{rg} = gas relative permeability

k_{rgb} = relative permeability of gas in the blockage region

k_{ro} = oil relative permeability

L = length, ft

L_{wh} = stabilized pipeline performance coefficient for pressure squared calculations, (MMscf-D/psia^{2n})

n = inverse slope (exponent) of deliverability curve

N_D = parameter used in the Gray correlation

N_k = parameter used to estimate relative oil volume for Region 2 Calculation

N_{Re} = Reynolds number

N_v = parameter used in the Gray correlation

p = pressure, psia

p^2 = pressure squared, psia^2

p^* = dewpoint of the wellstream, psia

p_c = wellhead shutin pressure, psia

p_d = dewpoint pressure, psia

p_{dwn} = downstream pressure, psia

p_p = gas pseudopressure, psia^2/cp

p_R = average reservoir pressure, psia

p_{sc} = pressure at standard conditions, psia

p_{sep} = separator pressure, psia

p_t = flowing tubinghead pressure, psia

p_{up} = upstream pressure, psia

p_w = wellhead static column flowing pressure, psia

p_{wf} = wellbore flowing pressure, psia

q = well surface gas rate, MMscf/D

r = pseudo wall roughness in Gray Correlation, in

r' = pseudo wall roughness for high liquid/gas ratios used in Gray Correlation, in

r_b = radius of blockage region, ft

r_e = well external drainage radius, ft

r_g = absolute roughness of pipe used in Gray Correlation, in

r_s = solution oil/gas ratio, STB/scf or STB/MMscf

r_w = wellbore radius, ft

R = ratio of liquid/gas superficial velocities used in Gray Correlation

R_p = producing gas/oil ratio, scf/STB or Mscf/STB

R_s = solution gas/oil ratio, scf/STB or Mscf/STB

s = skin factor, dimensionless

s_{cb} = skin due to condensate blockage

S = hydrostatic head term

S_o = oil saturation

S_{wi} = irreducible water saturation

T = temperature, °R

T_{in} = temperature of gas at inlet, °R

T_{sc} = temperature at standard conditions, °R

T_{wh} = stabilized tubing performance coefficient for pressure squared calculations, (MMscf-D/psia^{2n})

y_l = liquid holdup

v_m = mixture velocity, ft/s

v_{si} = superficial velocity of phase i, ft/s

V_g = gas volume, L^3, ft^3 or bbl

$V_{g,sc}$ = surface-gas volume, L^3, scf

V_{ro} = oil volume/oil volume at saturation pressure

z = gas "deviation" factor, or compressibility

α = constant in gas-condensate rate equation

γ_g = gas specific gravity (air = 1), dimensionless

γ_o = oil specific gravity (water = 1), dimensionless

ϵ = in-situ volume fraction of gas

θ = well deviation angle measured from vertical, degrees

λ_l = input fraction of liquid

μ_g = gas viscosity, cp

μ_o = oil viscosity, cp

ρ_g = gas density, lbm/ft^3

ρ_l = liquid density, lbm/ft^3

ρ_m = input fraction weighted density, lbm/ft^3

$\bar{\rho}$ = in-situ volume fraction of gas weighted density, lbm/ft^3

τ = interfacial tension, lb$_\mathrm{m}$/s^2

τ_o = gas/oil interfacial tension, lb$_\mathrm{m}$/s^2

τ_w = gas/water interfacial tension, lb$_\mathrm{m}$/s^2

τ_m = mixture interfacial tension, lb$_\mathrm{m}$/s^2

ϕ = porosity

Appendix A

Dry Gas VLP Model Used by Fetkovich

Mike Fetkovich used a variation of the *Average Temperature and z-Factor method* for determining the relationship between bottomhole flowing pressure p_{wf} and wellhead flowing tubing pressure p_t (Fetkovich, 1975).

$$p_{wf}^2 = e^S p_t^2 + \left(\frac{F_r q_g \bar{T} \bar{z}}{31.62}\right)^2 (e^S - 1), \tag{A.1}$$

where

$$F_r = \frac{0.10797}{D^{2.612}}. \tag{A.2}$$

The unit system is field units but the gas rate q_g is given in Mscf/D.
If we divide both sides by e^S and rearrange, we obtain

$$p_w^2 - p_t^2 = \left[\left(\frac{F_r \bar{T} \bar{z}}{31.62}\right)^2 \frac{(e^S - 1)}{e^S}\right] q_g^2 \tag{A.3}$$

From this equation we clearly see that for low pressure systems Δp^2 vs. q_g will yield a slope of 2, similar to the *Average Temperature and z-Factor method*.

Appendix B

Additional attachments

The following electronic documents are submitted as part of this thesis

- *Tore Nymoen MSc. project, Well Model.xlsm*

References

API (1978). *API Manual 14BM*. American Petroleum Institute, second edition. Appendix B: "Vertical Flow Correlation in Gas Wells".

BP (2017). Bp energy outlook, 2017 edition.

Economides, M. J., Hill, A. D., Ehlig-Economides, C., and Zhu, D. (2013). *Petroleum Production Systems*. Prentice Hall, 2 edition.

Fetkovich, M. (1973). The isochronal testing of oil wells. Paper SPE 4529 presented at the 48th Annual Fall Meeting of the Society of Petroleum Engineers of AIME, Las Vegas, NV, Sep. 30. - 03. Oct.

Fetkovich, M. (1975). Multipoint testing of gas wells. SPE Mid Continent Section Continuing Education Course, March 1975, Tulsa, OK.

Fevang, . and Whitson, C. (1995). Modeling gas condensate well deliverability. Paper SPE 30714 presented at the SPE Annual Technical Conference & Exhibition, Dallas, TX, 22-25 Octover.

Lee, J. and Wattenbarger, R. A. (1996). *Gas Reservoir Engineering*. SPE Textbook Series. Society of Petroleum Engineers.

Mott, R. (1999). Calculating well deliverability in gas condensate reservoirs. Presented at EAGE - 10th European Symposium on Improved Oil Recovery, Brighton, UK, 18-20 August.

Norsk Petroleum (2017). Eksportverdi av norsk petroleum, 1971-2016. Data gathered from Statistics Norway, Table 08800. Excel Sheet prepared by Norsk Petroleum `http://www.norskpetroleum.no/produksjon-og-eksport/eksport-av-olje-og-gass/`.

Oudeman, P. (2007). On the flow performance of velocity strings to unload wet gas wells. In *SPE Middle East Oil and Gas Show and Conference*. Society of Petroleum Engineers (SPE).

Oyewole, A. (2015). Extension of the gray correlation to inclination angles. In *SPE Annual Technical Conference and Exhibition*. Society of Petroleum Engineers (SPE).

Petrowiki (2015a). Gas well deliverability. `http://petrowiki.org/Gas_well_deliverability` (Accessed 05.11.2016).

Petrowiki (2015b). Pressure drop evaluation along pipelines. `http://petrowiki.org/Pressure_drop_evaluation_along_pipelines` (accessed 09.11.2016).

Petrowiki (2015c). Wellbore flow performance. `http://petrowiki.org/Wellbore_flow_performance` (accessed 07.11.2016).

Pope, G., Wu, W., Narayanaswamy, G., Delshad, M., Sharma, M., and P, W. (2000). Modeling relative permeability effects in gas-condensate reservoirs with a new trapping model. *SPE Reservoir Evaluation & Engineering*, 3(2):171–178.

Whitson, C. and Brulé, M. (2000). *Phase Behavior*. SPE Monograph Series, Volume 20. Society of Petroleum Engineers.

Wikipedia (2017). Visual basic for applications. `https://en.wikipedia.org/wiki/Visual_Basic_for_Applications` (accessed 11.05.2017).

Øyvind Fevang (1995). *Gas Condensate Flow Behavior and Sampling*. PhD thesis, NTH (Now NTNU).